Hindawi
Complexity
Volume 2023, Article ID 5557123, 20 pages
https://doi.org/10.1155/2023/5557123

Research Article

Transition Yet Energy Consuming for Tumor Growth Regulated by the Colored Microenvironment

Leiyan Chen,[1,2] Yan Wang,[3] Qingqing Li,[4] and Haohua Wang [1,5]

[1]*School of Mathematics and Statistics, Hainan University, Haikou 570228, Hainan, China*
[2]*School of Mathematics, Sun Yat-Sen University, Guangzhou 510275, China*
[3]*Department of Neurology, The First Affiliated Hospital, University of South China, Hengyang 421001, Hunan, China*
[4]*School of Computer Science and Technology, Dongguan University of Technology, Dongguan 523808, China*
[5]*Hainan University, Key Laboratory of Engineering Modeling and Statistical Computation of Hainan Province, Haikou 570228, Hainan, China*

Correspondence should be addressed to Haohua Wang; huazi8112@hainanu.edu.cn

Received 15 July 2023; Revised 13 November 2023; Accepted 21 November 2023; Published 13 December 2023

Academic Editor: Wen-Long Shang

Transition or metastasis is a main characteristic of tumor developmental processes. However, the mechanism behind the transition and what costs involved are obscure when the tumor is exposed to a colored microscopic environment. Here, focusing on the regulatory role of noises from its strength and correlation time on phenotypic diversity of tumors, we show that (1) when the noise strength (NS) is fixed, extending the autocorrelation time (AT) of multiplicative noise can regulate bidirectionally the tumor phenotype, i.e., it can promote the diffusion also contribute to killing cancer cells simultaneously; (2) AT of additive noise can reduce the occurrence probability of cancer cells, but the NS can increase this probability; (3) the effect of the cross-correlated strength (CS) on cell phenotype is twofold, i.e., increasing CS may urge the mean first passage time (MFPT) of switching to the tumor state to have the minimum and maximum values but the cross-correlation time (CT) always makes the MFPT to have a minimum value. In addition, NS can make MFPT to have a peak. Moreover, by reconstructing the reaction network from the mesoscopic scale, we further show that AT of multiplicative noise can increase energy consumption, and there exists a trade-off between NS and AT of additive noise. We also show that the energy consumption is monotonically decreasing with increasing the CT but the CS can amplify the difference of this dependence. The overall analysis implies that tumor cells would make use of external noise to survive in fluctuating environments.

1. Introduction

Transition or phenotypic switching is a remarkable characteristic of tumors. After undergoing multistep processes so-called invasion-metastasis cascade, the tumor achieves metastasis and propagates from primary tumor cells to distant organs [1–4]. Primary tumor cells first locally invade normal tissues surrounding them and then will proliferate and colonize at a distant site by intravasation into and extravasation from the systemic circulation; here, the metastatic cells also depend on an often-foreign cell microenvironment [5–7], in which environmental factors often play critical roles in the sense of stochastic bifurcation by regulating each biochemical step of the tumor cell development, including mediating local invasion, cooperating some competing endogenous, and activation of the signal pathway. Much progress has been made in understanding the relationship between tumor transition and environmental white fluctuations (a classical framework of thermodynamic fluctuations or Brownian motions [8–11]). However, the correlation between internal and external stochastic fluctuations has a substantial time comparable to the cell cycle (these fluctuations are always called "colored") [12–15], and their interplay interferes with classical thermodynamic equilibrium. Despite this general description, how the process of tumor transition and metastasis is

achieved and how much energy it costs are all elusive, moreover, the roles of regulation from colored noise sources in tumor development, including the interactions of AT/CT (auto/cross-correlation time) of colored noises, remain not fully understood.

In general, cell fate and decision are determined by cellular phenotype defined as the number of peaks in the steady distribution of attractors in a phase plane, and tumor cell development will switch between these attractors in line with stochastic bifurcation regulated by the fluctuation microenvironment [16, 17]. In the landscape of tumor development, the attractor may exist in a discrete form in space, and the tumor cell fate depends on the dwell time of each attractor, which is a main source of stochasticity or noise [18–20]. The classical thermodynamic balance follows the classical Markov assumption and ubiquitous principle; that is, the dwell time of the system in every attractor follows exponential distribution and has no memory [21–24]. However, the results of recent biological experiments on cancer metastasis have indicated that the long noncoding RNA (lncRNA) MALAT1 regulates tumor differentiation (as evidenced by cystic and encapsulated tumor appearance) by localizing to nuclear speckles and altering transcription based on initial descriptions [25–27]. The fluctuations in the abundance of MALAT1 form an external signal to regulate the system dwell time into a nonexponential distribution and then alter the promoter activity, resulting in the memory (self-autocorrelation). This implies that the gene expression noise is in nature colored (i.e., the noise has nonzero correlation time) [26, 28]. From the perspective of biological function, Shahrezaei and Swain verified that the memory from colored noise can improve response sensitivity, by amplifying stochasticity in coherent feedforward loops while attenuating noise in incoherent feedforward loops [22]. This means that the AT/CT may act as a "fine-tuner" of complex cellular systems to regulate cell phenotype and transition. Essentially, the colored fluctuation environment breaks the Markov assumption, leading to a non-Markovian jump process. Deciphering effectively how the AT/CT regulates cell phenotype switching is an important and challenging task [29–31]. Fortunately, Novikov's theorem provides an excellent method to transform a complex system embedding in a colored microscopic environment into the Markov jump process to address the effect of the AT/CT on cell phenotypic diversity, which is more directly effective than the stationary generalized chemical-master equation (sgCME) [30, 32–34]. Hence, it is significant to study the effect of colored noise (focusing on AT/CT regulation from the time viewpoint) on tumor cell transition.

Essentially, the existence of AT/CT may induce the change of dwell time of every attractor and render the jump process between distinct attractors to produce the molecular memory, breaking the detailed balance in tumor development. These transitions between metastable states need to dissipate the free energy [35–39]. Here, free energy is a physical concept described as the work done by the transport of a bead from one well to the other and back, measured by entropy production that illustrates the irreversibility of the jump stochastic process according to Landauer's principle [40–43]. The decomposition of circumfluence is a key step for calculating entropy production. However, in the tumor development process, AT/CT of fluctuations originating from the abundance of MALAT1 may have a nonzero time lag in every attractor, rendering cycle flow decomposition difficult. Here, investigating the equivalence from the mesoscopic scale, we propose the approximation algorithm to estimate the equivalent switching rate among the distinct attractors by employing the technology of a linear mapping approximation [40, 41, 44, 45]. The advantage of this algorithm is that we can yield directly the probability net flux of every attractor but also obtain the entropy production rate for a given complex multistable system [44, 45]. Therefore, clarifying how much free energy is consumed from the viewpoint of nonequilibrium and emphasizing the regulated function of AT/CT for achieving tumor cell transition and metastasis are important for dynamic intervention in tumor development.

Inspired by the significant experiments on the lncRNA MALAT1in lung cancer metastasis [26, 46], we introduce a mechanistic model with a colored microenvironment due to fluctuations in the abundance of MALAT1 to emphasize the regulation of AT/CT on tumor transition and metastasis. Moreover, we mainly focus on the mechanism of how to achieve the biological function (phase switching) and what cost is involved, beyond the previous reports only on the stochastic resonance [47, 48]. According to the dynamic analysis in multitime scales, we could uncover that the AT/CT and NS/CS can regulate tumor cell dynamic evolution process determined largely by the types of noise. For the landscape of tumor development, amplifying the NS of additive noise can suppress tumor cell metastasis, while enhancing the AT of multiplicative noise may have a dual function, that is, it can not only induce the tumor cell switching but also promote the killing of cancer cells; The biological function is achieved by mediating the stochastic bistability regime triggered by the NS and AT. The CS of the noises can also have a double function, depending on positive or negative values, i.e., enhancing the CS (from a negative correlation to a positive correlation) can induce the MFPT from the primary tumor to the malignant tumor to have a minimum value and a maximum value, but the CT always has a minimum value. More importantly, the development state of tumor cells jumping between distinct attractors needs to dissipate more energy with increasing the CT in a multiplicative environment, and there exists a trade-off by regulating NS and AT in the additive noisy environment. In addition, the energy consumption is monotonically decreasing with increasing CT, and the CS can promote this dependence relationship.

This, then, signal sensing is the most ubiquitous process in tumor cell development, the question of what mechanism is behind the complex regulation, including how to induce the phenotypic switching in a noisy environment and what cost to consume, is all not previously known. Focusing on these hotspots is important for elucidating the mechanism of tumor cell metastasis and dynamic evolution.

2. Model and Methods

2.1. Model Description. Here, considering the attack of immune cytotoxic cells, we model the growth process of cancerous tissue, to focus on the NS and AT/CT of the colored stochastic fluctuations, on tumor cell development. It is known that, due to the existence of the immune T lymphocytes (effector cells), the development of reducing tumor cells (target cells) may be simulated as a biochemical process including the following reactions [49, 50]:

$$\begin{aligned} \text{Normal Cells} &\xrightarrow{A} X \\ X &\xrightarrow{\lambda} 2X \\ X + E_0 &\xrightarrow{k_1} E \xrightarrow{k_2} E_0 + P \\ P &\xrightarrow{k_3} \phi, \end{aligned} \tag{1}$$

where X denotes the tumor cell that proliferates spontaneously at a rate λ, and their local interactions with cytotoxic cells E_0 (effector cells) are illustrated by a kinetics parameter k_1, implying the rate of binding of immune cells to the complex E that subsequently dissociates at a rate k_2, refer to Figure 1. Also, this dissociation results in a product P that represents dead or nonreplicating tumor cells. k_3 is the degradation rate of P and A is the normal cell carnification coefficient. This simple motif, which can be used to model many motifs in response to various possible cell microenvironments [51–53], has been extensively studied.

To introduce noisy sources in the above tumor-growth model, we simply introduce the background of the small molecule MALAT1 of the lncRNAs, the first one found in cancer metastasis. This small molecule is the main biomarker cell in lung cancer metastases [2, 25] and can regulate tumor differentiation (e.g., the development of cystic and encapsulated tumor appearance) by localizing to nuclear speckles. Recent experimental results have indicated that in the mouse mammary tumor virus-(MMTV-) polyomavirus middle T antigen (PyMT) model of human luminal B breast cancer, promoter deletion or ASO-mediated knock-down of MALAT1 can result in the decrease of lung metastases and the elevation of E-cadherin (supporting an epithelial phenotype). Most cancer cells are likely kept in blood vessels compared with control cells, implying that the cancer cells do not invade distal lung sites form micrometastases, i.e., ineffective colonization following MALAT1 knockout [7, 46], and also implying that the tumor cell transition is indeed due to the colored noise from fluctuations in the MALAT1 abundance (specifically, these fluctuations are due to lncRNA MALAT1 localizing to nuclear speckles and may be modeled as dichotomous noise that has been proved to have some memory [54, 55]). Here, we try to answer the traditional issues of whether noise is harmful or beneficial for cell development, emphasizing how AT/CT and NS affect the phenotype shift and metastasis of tumor cells.

2.2. Mathematical Models. Without loss of generality, the number of immune cells satisfies the conservative condition: $E_0 + E = E_1$. Then, the tumor development described by equation (1) is essential in a series of ordinary differential equations (ODEs) that demonstrates the transient evolution process of each species (for more details, refer to Appendix A).

$$\begin{aligned} \frac{\mathrm{d}X}{\mathrm{d}t} &= A(N - X) + \lambda X - k_1 E_0 X, \\ \frac{\mathrm{d}E_0}{\mathrm{d}t} &= -k_1 E_0 X + k_2 (E_1 - E_0), \\ \frac{\mathrm{d}P}{\mathrm{d}t} &= k_2 (E_1 - E_0) - k_3 P, \end{aligned} \tag{2}$$

where N stands for the maximum number of normal cells, the resulting kinetics can be dimensionless directly by setting $\lambda t \longrightarrow t, k_1 X/k_2 \longrightarrow x, k_1 P/k_2 \longrightarrow z, E_0/E_1 \longrightarrow y$, $k_3/\lambda = a, k_2/k_1 = \theta, k_1 E_1/\lambda = \beta$, $\lambda X(1 - \theta X)/N - X = A, k_2/\lambda = c$, and equation (2) has the following equivalent forms:

$$\begin{aligned} \frac{\mathrm{d}x}{\mathrm{d}t} &= x(1 - \theta x) - \beta \mathrm{xy}, \\ \frac{\mathrm{d}y}{\mathrm{d}t} &= c(1 - y - \mathrm{xy}), \\ \frac{\mathrm{d}z}{\mathrm{d}t} &= \beta(1 - y) - \mathrm{az}. \end{aligned} \tag{3}$$

In general, the parameter $\beta > 1$ holds, meaning that the product of the rate of effector cell binding to cancer cells, and gives a general assumption that the total number of conjugate cells per unit volume is greater than the rate of cancer cell proliferation. Therefore, we can divide the whole tumor cell development network into three types of motif: recognition, apoptosis procedure, and apoptosis [1, 3, 4, 56], meaning there may be a huge difference in time scale between the three processes. We also can treat the system as the coupled of fast and slow subsystems [42, 57–61]. According to the method of separating time scales and quasi-steady-state approximation [31], we can yield a steady probability distribution for biomarker protein (Figure 1(a)). Here, we emphasize mainly the concentration of the tumor cells. Let the second and third of (3) be equal to zero, we can easily get the expressions of steady state y, z in terms of x. If these expressions are substituted into the slow equation, then we yield the following reduced system (for more details, refer to Appendix A):

$$\frac{\mathrm{d}x}{\mathrm{d}t} = x(1 - \theta x) - \beta \frac{x}{x + 1} \triangleq f(x), \tag{4}$$

where x represents the actual concentration of the tumor cell, β is the immune rate, and θ is the constant parameter. Obviously, this motif, coupling a positive and negative feedback loop, would have two steady states depending on different parameter values. In addition, the deterministic potential function defined by the deterministic force $f(x)$ in (4) is given by

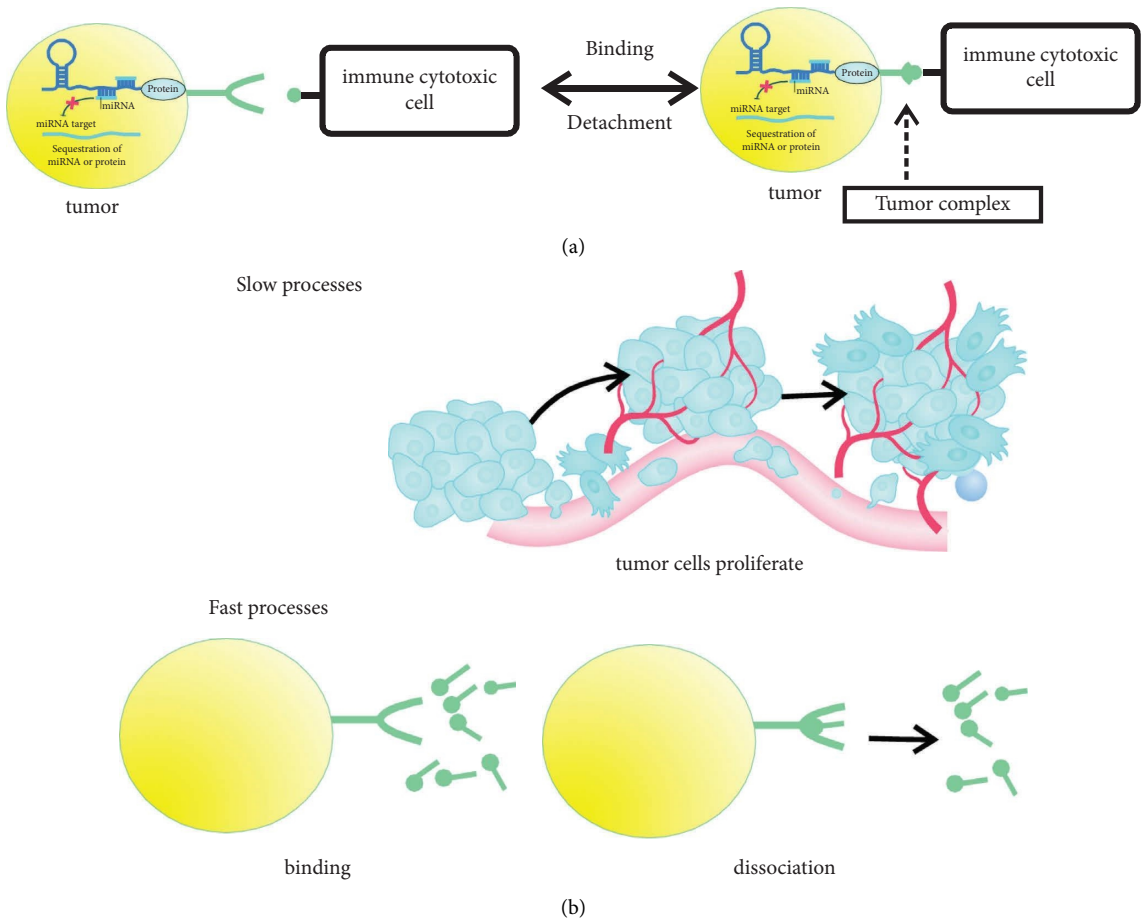

FIGURE 1: The schematic diagram of tumor development in a colored noise environment. (a) Tumor cells' interaction with cytotoxic cells and the formation of the proliferation complex are regulated by the lncRNAs throughout the expression process; (b) separating the tumor cell progress into the fast and slow processes (reaction rates not shown).

$$V(x) = -\int f(x)\mathrm{d}x = -\frac{x^2}{2} + \frac{\theta x^3}{3} + \beta x - \beta \ln(x+1), \tag{5}$$

from which we obtain two steady attractors $x_1 = 0$ (the extinction state of the tumor) and $x_2 = x_s = (1-\theta+\sqrt{(1+\theta)^2 - 4\beta\theta})/2\theta > 0$ (the stable state of the tumor), and one unstable steady state $x_u = (1-\theta-\sqrt{(1+\theta)^2 - 4\beta\theta})/2\theta$.

Of note, the system parameters are set according to the recent experiment on lung cancer evolution [26], and the values are listed in the note of numerical results. Using these data, we can show that there are two stable attractors in the given system and its potential function has double wells (Figure 2). These two stable steady states correspond, respectively, to the tumor cell extinction state ($x_1 = 0$) and the stable tumor state ($x_2 = 7.2659$), and the unstable state 1.7341. Moreover, the system has a bistable region in the space of parameters.

Next, we introduce a stochastic model. Of note, the stochastic environment originating from the fluctuations in the MALAT1 will directly influence the tumor number and alter the tumor's immune rate, being the main source of extrinsic noise. Also, this extrinsic noise may be colored noise for the reasons stated above. The fluctuations affecting the immune rate β result in multidimensional noises, that is, additive noise $\eta(t)$ and multiplicative noise $\mathrm{d}x/\mathrm{d}t = x(1-\theta x) - \beta x/x + 1 - x/x + 1\xi(t) + \eta(t)$, which can be viewed as the capability for expansionary transfer of the tumor cells. The consideration of these factors combined with deterministic equation (4) leads to the more complex forms as follows:

$$\frac{\mathrm{d}x}{\mathrm{d}t} = x(1-\theta x) - \beta\frac{x}{x+1} - \frac{x}{x+1}\xi(t) + \eta(t). \tag{6}$$

In equation (6), two noises are all assumed to be Gauss-colored noises and nonzero autocorrelation, that is,

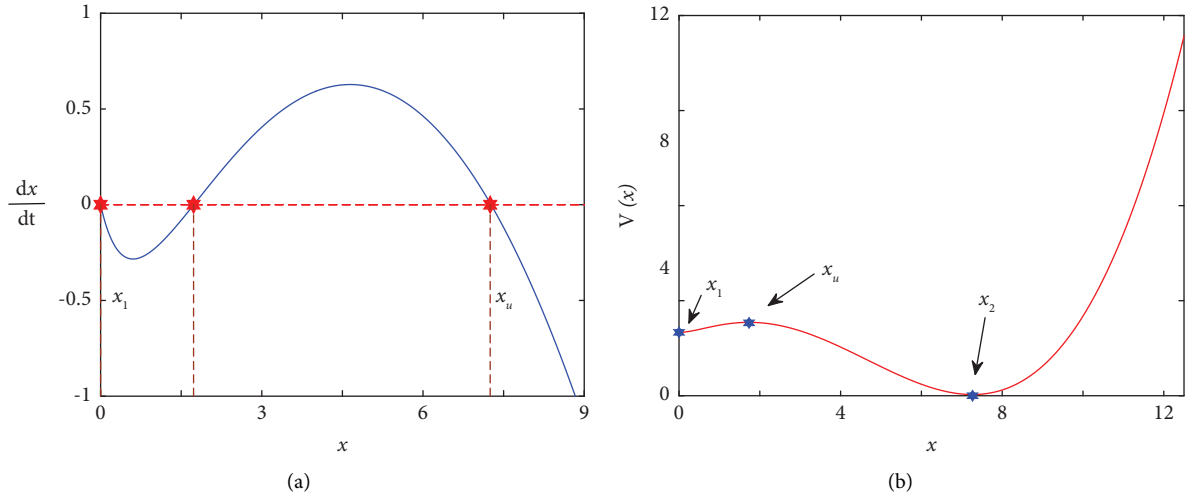

FIGURE 2: The steady-state solution (x_i) of tumor cell development (a) and the potential function (b). The parameters are from the experiment on lung cancer [26], and $\theta = 0.1$ s-1copy-1 and $\beta = 2.26$ s-1copy-1. Here, $x_1 = 0$ nm is the extinction state of the tumor cell, $x_2 = 7.2659$ nm represents the tumor state, and $x_u = 1.7341$ nm is the transient state.

$$\begin{aligned}
\langle \xi(t) \rangle &= \langle \eta(t) \rangle = 0, \\
\gamma_{11}(t, t+\Delta t) &= \langle \xi(t)\xi(t+\Delta t) \rangle = \frac{D}{\tau_1} \exp\left(-\frac{|\Delta t|}{\tau_1}\right), \\
\gamma_{22}(t, t+\Delta t) &= \langle \eta(t)\eta(t+\Delta t) \rangle = \frac{\alpha}{\tau_2} \exp\left(-\frac{|\Delta t|}{\tau_2}\right), \\
\gamma_{12}(t, t+\Delta t) &= \gamma_{21}(t, t+\Delta t) = \langle \xi(t)\eta(t+\Delta t) \rangle \\
&= \langle \eta(t)\xi(t+\Delta t) \rangle = \frac{\lambda D\alpha}{\tau_3} \exp\left(-\frac{|\Delta t|}{\tau_3}\right).
\end{aligned} \tag{7}$$

Here, symbol $\langle \cdot \rangle$ represents the mean or expectation, Δt is the time window, τ_1, τ_2 are AT, D, α are the NS, and λ, τ_3 are CS and CT, of the corresponding noise process.

Note that equation (6) is used to describe the tumor development as shown in Figure 1. The existence of colored noise embedded in tumor development impels the dwell time in each attractor to drift from the classical Markov assumption; that is, it is impossible to obtain directly the stationary probability distribution by the two types of the classical stochastic integral. Obviously, the dwell time in each attractor of nonexponential distribution means that the gene expression must have some so-called molecular memory [26, 28, 30–32]. In particular, if $\tau_i \longrightarrow 0$, the colored noise degenerates directly into the Gaussian white noise, and we can solve the above equation by the Ito stochastic integral. In fact, analytical results were obtained for similar cases [31, 62–64]. Here, we investigate mainly the biological function of colored noise, i.e., the effects of this noise on phenotypic transition and stability of tumor cells.

3. Main Results

3.1. Analytical Results: The Steady Distribution and Its Peaks. Generally, a cell's phenotype may be partly reflected by the number of peaks and their steep degrees in a stationary probability distribution. Considering the influence of the noisy environment on tumor cell development, we employ Novikov's theorem [65, 66] to transform the non-Markov process into the approximation Fokker–Planck equation (aFPE) to emphasize the regulation of AT on tumor phenotype [65, 66]. According to equations (6) and (7), we can derive an aFPE (refer to Appendix B for derivation).

$$\begin{aligned}\frac{\partial}{\partial t}P(x,t) = &-\frac{\partial}{\partial t}\left[x(1-\theta x)-\beta\frac{x}{x+1}\right]P(x,t)\\ &+\frac{D}{1-\tau_1\left[f^{'}(x_s)-f(x_s)g_1'(x_s)/g_1(x_s)\right]}\frac{\partial}{\partial x}g_1(x)\frac{\partial}{\partial x}g_1(x)P(x,t)\\ &+\frac{\lambda\sqrt{D\alpha}}{1-\tau_3\left[f^{'}(x_s)-f(x_s)g_2'(x_s)/g_2(x_s)\right]}\frac{\partial}{\partial x}g_1(x)\,\frac{\partial}{\partial x}g_2(x)\,P(x,t)\\ &+\frac{\alpha}{1-\tau_2\left[f^{'}(x_s)-f(x_s)g_2'(x_s)/g_2(x_s)\right]}\frac{\partial}{\partial x}g_2(x)\frac{\partial}{\partial x}g_2(x)P(x,t)\\ &+\frac{\lambda\sqrt{D\alpha}}{1-\tau_3\left[f^{'}(x_s)-f(x_s)g_1'(x_s)/g_1(x_s)\right]}\frac{\partial}{\partial x}g_2(x)\,\frac{\partial}{\partial x}g_1(x)\,P(x,t),\end{aligned} \tag{8}$$

where $g_1(x) = -x/x+1$ and $g_2(x) = 1$; $f(x) = x(1-\theta x) - \beta x/x+1$, $f^{'}(x_s) = f^{'}(x)|_{x=x_s}$ denotes the derivation of force at the attractor x_s, and it must satisfy the inequality $1-\tau_i[f^{'}(x_s) - f(x_s)g_j'(x_s)/g_j(x_s)] > 0$ $(i,\ j=1,\ 2,\ 3)$ that limits the ranges of the correlation times, and

$$\begin{aligned}f(x_s) &= x_s(1-\theta x_s) - \beta\frac{x_s}{x_s+1},\\ f^{'}(x_s) &= (1-2\theta x_s) - \beta\frac{1}{(x_s+1)^2}.\end{aligned} \tag{9}$$

Equation (8) can be rewritten as

$$\frac{\partial P(x,t)}{\partial t} = -\frac{\partial}{\partial x}A(x)P(x,t) + \frac{\partial^2}{\partial x^2}B(x)P(x,t), \tag{10}$$

where

$$\begin{aligned}A(x) = &\ x(1-\theta x) - \beta\frac{x}{x+1} + \frac{D}{1-\tau_1C_1}\frac{x}{(x+1)^3}\\ &-\lambda\sqrt{D\alpha}C_3\frac{1}{2(x+1)^2},\end{aligned} \tag{11}$$

$$B(x) = \frac{D}{1-\tau_1C_1}\left(\frac{x}{x+1}\right)^2 - \lambda\sqrt{D\alpha}C_3\frac{x}{x+1} + \frac{\alpha}{1-\tau_2C_2}, \tag{12}$$

with

$$\begin{aligned}C_1 &= f^{'}(x_s) - \frac{f(x_s)}{x_s(x_s+1)},\\ C_2 &= f^{'}(x_s),\\ C_3 &= \frac{1}{1-\tau_3C_1} + \frac{1}{1-\tau_3C_2}.\end{aligned} \tag{13}$$

According to equations (10)–(13), the steady distribution $P_{st}(x)$ satisfying condition $\lambda < 2/\sqrt{(1-\tau_1C_1)(1-\tau_2C_2)}C_3$ takes the form

$$\begin{aligned}P_{st}(x) &= \frac{N}{B(x)}\exp\int^x\frac{A(x')}{B(x')}\mathrm{d}x'\\ &= \frac{N}{B^{1/2}(x)}\exp\left[-\frac{U(x)}{D}\right],\end{aligned} \tag{14}$$

where N is a normalization constant and the stochastic potential function x_u is given by

$$U(x) = -\int^x\frac{x(1-\theta x)-\beta(x/x+1)}{1/1-\tau_1C_1(x/x+1)^2 - \lambda\sqrt{\alpha/D}C_3(x/x+1) + (\alpha/D)/1-\tau_2C_2}\mathrm{d}x. \tag{15}$$

From this equation, we can obtain the following explicit expression of $\mathrm{d}P_{st}(x)/\mathrm{d}x = 0$:

$$U(x) = \frac{\theta(1-\tau_1 C_1)}{3m}x^3 + \frac{1-\tau_1 C_1}{2m}\left(2\theta - 1 - \frac{n}{m}\theta\right)x^2 - \frac{\gamma_1}{m}(1-\tau_1 C_1)x + \frac{1-\tau_1 C_1}{2m}\left(\gamma_2 - \frac{n}{m}\gamma_1\right)\ln\left|x^2 + \frac{n}{m}x + \frac{R}{m}\right| - \frac{2\gamma_3(1-\tau_1 C_1)}{\sqrt{4mR - n^2}} \times \arctan\frac{2mx+n}{\sqrt{4mR-n^2}}, \tag{16}$$

where

$$R = \frac{\widetilde{\alpha}}{\widetilde{D}}, \widetilde{D} = \frac{D}{1-\tau_1 C_1}, \widetilde{\alpha} = \frac{\alpha}{1-\tau_2 C_2},$$
$$\widetilde{\lambda} = \sqrt{(1-\tau_1 C_1)(1-\tau_2 C_2)}C_3\lambda,$$
$$m = 1 - \widetilde{\lambda}\sqrt{R} + R, n = 2R - \widetilde{\lambda}\sqrt{R},$$
$$\gamma_1 = \beta - 2 + \theta - \frac{R}{m}\theta - \left(2\theta - 1 - \frac{n}{m}\theta\right)\frac{n}{m},$$
$$\gamma_2 = \beta - 1 - \left(2\theta - 1 - \frac{n}{m}\theta\right)\frac{R}{m},$$
$$\gamma_3 = \frac{\gamma_1}{m}R + \frac{n}{2m}\left(\gamma_2 - \frac{n}{m}\gamma_1\right). \tag{17}$$

The stochastic potential given by equation (16) can provide the information of stability of the corresponding probability distribution, similar to the case of the potential of the deterministic system described by equation (5). Here, we are interested in understanding how colored noise can induce the transition between stationary states. For the deterministic system described by equation (4), this induction can be achieved by analyzing the existence of a critical point or bifurcation point (x_u) and its stability in a given parameter interval. In the stochastic case, however, the stability of the steady distribution can be illustrated by the number of peaks of the corresponding stochastic potential function, obtained from the equation $dP_{st}(x)/dx = 0$ [9]. Moreover, we find that the bifurcation condition can also be written as the following algebraic equation:

$$x(1-\theta x) - \beta\frac{x}{x+1} - \frac{D}{1-\tau_1 C_1}\frac{x}{(x+1)^3} + \frac{\lambda\sqrt{D\alpha}}{1-\tau_3 C_2}\frac{1}{(x+1)^2} = 0. \tag{18}$$

3.2. Tumor Phenotypic Diversity from the Interplay of AT/CT and NS. The tumor development process is essentially noisy and exhibits distinct phenotypes. Recently, the results on lncRNA MALAT1 have indicated that correlation function AT/CT is changeable, implying that we can use this changeable AT/CT in tumor development to achieve phenotypic diversity [67, 68]. In order to investigate the regulation effect of colored noise (i.e., $D, \alpha, \lambda, \tau_1, \tau_2$, and τ_3) on state transition, we analyze the equations of probability distributions (i.e., equations (10)–(15)). For clarity, we distinguish three types of cases: (i) the noise is present only in the immune rate, i.e., only multiplicative noise; (ii) only additive noise; (iii) two kinds of noisy sources are simultaneously present. In Table 1, we present these three cases of the parameter values.

3.2.1. Effect of Multiplicative Noise on State Transition. Here, we consider that the correlated Gaussian noise $\xi(t)$ appears in the immune rate in equation (6), i.e., the corresponding stochastic equation takes the form

$$\frac{dx}{dt} = x(1-\theta x) - [\beta + \xi(t)]\frac{x}{x+1}. \tag{19}$$

From this equation, we can show that a small fluctuation in the immune rate may result in a sudden transition because of the appearance of multiplicative noise. Fixed control parameters θ and β, changing the multiplicative noise $\xi(t)$, may reshape the phenotype of stationary probability distribution (equation (14)), referring to Figure 3. This figure demonstrates that the steady distribution $P_{st}(x)$ that is in the form of a function of the density of tumor cell x may change its shape with changing the colored noise environment. Specifically, the probability of a stable tumor state (high state) reduces with increasing AT (the blue to green line), implying that increasing the AT may help to kill the cancer cell. Meanwhile, the probability at extinction state (low state, i.e., $x = 0$) falls rapidly. In Figure 3(b), the AT has a similar but more significant effect on the stationary probability distribution when the NS increases from 0.2 to 0.7. This means that a larger NS can amplify the effect of AT on cell phenotype. In fact, comparing Figures 3(a) with 3(b), it is obvious that the probability of the unstable attractor increases gradually with increasing the AT, and the NS can make this difference more apparent, implying that the AT is a main factor promoting the tumor cells to diffuse and the NS accelerates the diffusion. In a word, the multiplicative noise may have a dual function in tumor cell development when the AT and NS change; that is, it can promote directly tumor cell diffusion and also contribute to killing the tumor cells at the same time.

From equations (18) and (19), we can show that the extremum values of the steady distribution satisfy the following condition:

$$x(1-\theta x) - \beta\frac{x}{x+1} - \frac{D}{1-\tau_1 C_1}\frac{x}{(x+1)^3} = 0. \tag{20}$$

According to this equation, we plot the extremum of the stationary probability distribution function as a function of the immune rate β as shown in Figure 4.

After determining the extrema of the stationary distribution function, we next investigate critical transition (i.e., find the tipping point at which abrupt state changes in the tumor cell development), which can be achieved by changing AT and NS. Figure 4 indicates that the effect of the NS and AT on the stationary distribution is nearly opposite [70]. Specifically, when the AT is fixed at 0.01, increasing the

Table 1: Parameter values of colored noise correspond to three types of cases: case (i) only multiplicative noise, case (ii) only additive noise, and case (iii) the mixture of multiplicative noise and additive noise.

Parameters	D	α	λ	τ_1	τ_2	τ_3
Case (i)	≠0	=0	=0	≠0	=0	=0
Case (ii)	=0	≠0	=0	=0	≠0	=0
Case (iii)	≠0	≠0	≠0	≠0	≠0	≠0

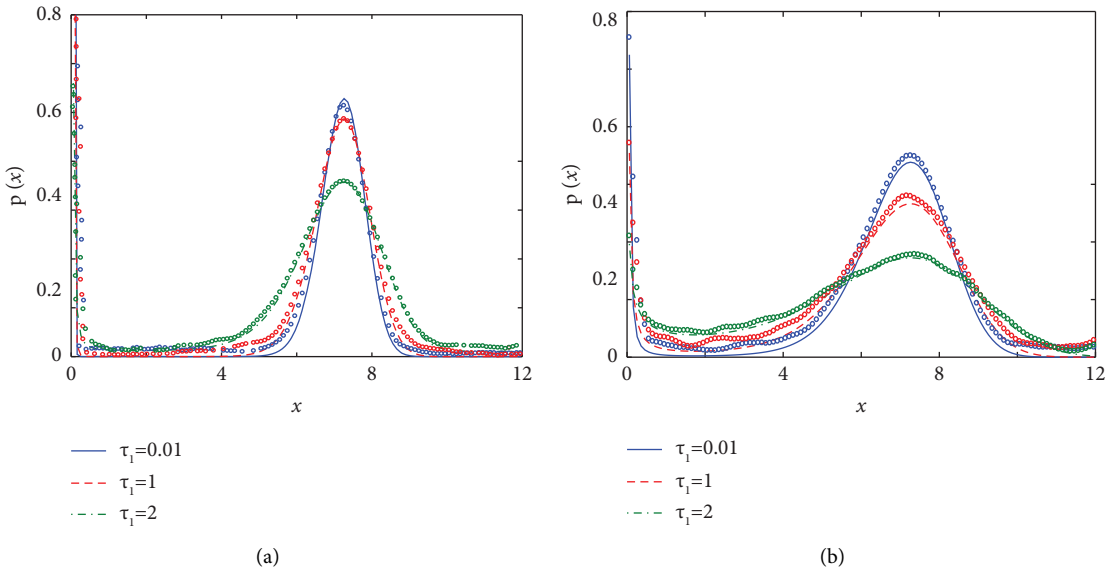

Figure 3: The regulation of the AT and NS as functions of the density of tumor cells on the stationary probability distribution in a multiplicative noise environment. (a) If the NS is fixed at 0.2, the AT increases from 0.01 to 2; (b) if the NS is fixed at 0.7, the AT increases from 0.01 to 2. The circle line represents the stochastic simulation [69]. The other parameter values are $\theta = 0.1\, s^{-1}\text{copy}^{-1}$ and $\beta = 2.26\, s^{-1}\text{copy}^{-1}$, which satisfy the bistable condition in Figure 2.

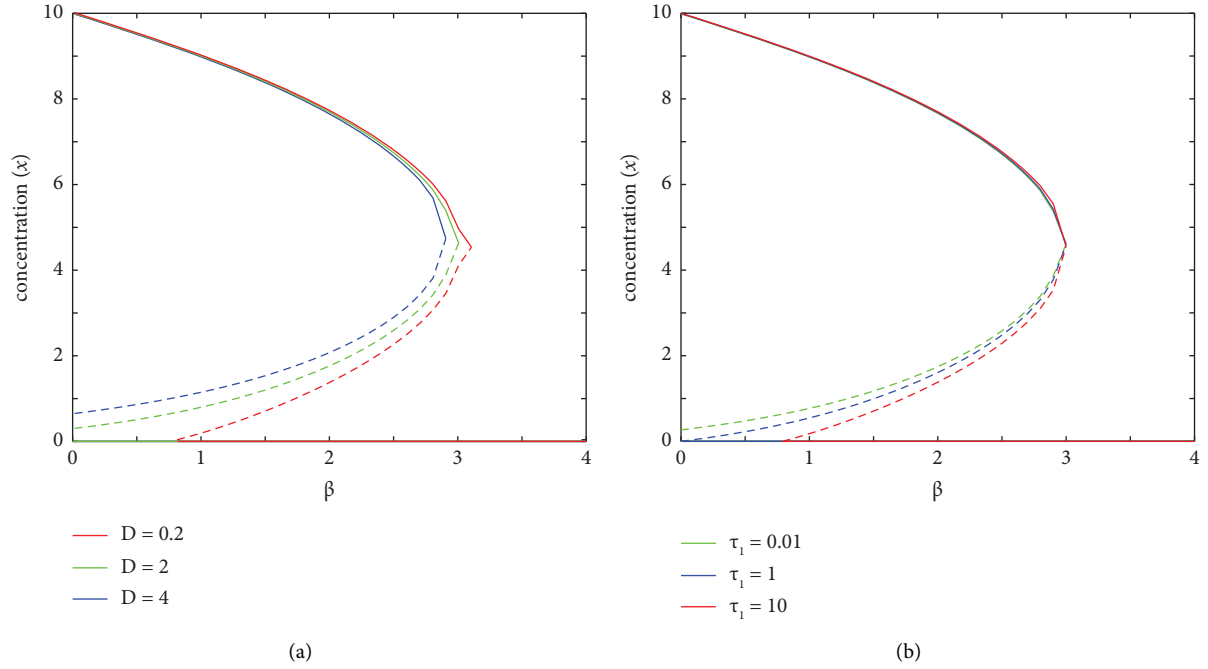

Figure 4: Extrema of the steady distribution of the model (19) subjected to the noise only in the immune rate β, i.e., only multiplicative noise is considered. (a) For a fixed AT $\tau_1 = 0.01$, increasing the NS from 0.2 to 2 to 4 (from red line to green line to blue line); (b) for a fixed NS $D = 2$, increasing the AT from 0.01 to 1 to 10 (from green line to blue line to red line). The other parameter value is $\theta = 0.1\ \text{s}^{-1}\text{copy}^{-1}$, and the dashed line denotes an unstable attractor.

NS from 0.2 to 2 to 4 (referring to Figure 4(a), from red line to green line to blue line) may broaden the bistable regime due to changes in the position of the unstable attractor (refer to the dashed line). This would hint that the fact that the regulation of the NS may be equivalent to that of positive feedback in the case of gene expression since positive feedback may induce bistability [30]. However, the way of phenotype diversity by regulating AT would be different. Figure 4(b) shows that when the NS is fixed at 2, the bistable regime of the underlying system reduces with increasing the AT from 0.01 to 1 to 10 (referring to Figure 4(b), from green line to blue line to red line), implying that the AT may attenuate the regulation of NS. Therefore, the AT and NS of colored noise may have a hedge in regulating the bistable regime of the tumor development system. Comparing Figures 4(a) with 4(b), it is clear that the high state (tumor state) and the low state (extinction state) are nearly unchanged and the zero is always a stable attractor of the system due to the structure of equation (19). The unstable state in tumor development is transient, implying that this transient state may switch not only to extinction state (low state) but also to tumor state (high state) in a given level of probability, depending on the type of noise, and the AT and NS may mediate the probability of achieving the tumor cell diffusion or vanishing, thus explaining why the multiplicative noise has a dual function in tumor cell development.

3.2.2. Effect of Additive Noise on State Transition. In contrast to the case of multiplicative noise, we can more directly show the biological function of additive noise. Keeping the NS fixed and increasing the AT reduce substantially the probability of tumor state but increase the probability of extinction state (Figure 5), implying that the regulation of AT in an additive noisy environment may inhibit the development of tumor cells. However, upon combining Figures 5(a) with 5(b), it can be observed that the changing trend of the stationary probability distribution is nearly the same even if the NS changes from 0.2 (Figure 5(a)) to 0.7 (Figure 5(b)), and the probability of extinction state shows a larger increase in Figure 5(a) than that is in Figure 5(b), indicating that when the NS is small, the phenotype of the system is more sensitive to the AT, and the NS may attenuate the effect of the AT.

3.2.3. Joint Effect of Multiplicative and Additive Noise on State Transition. Here, we analyze the Langevin equation (6) where multiplicative noise and additive noise are simultaneously present, i.e., Case (iii). In this case, we need to consider the CT λ between multiplicative noise and additive noise. This consideration involves feedback regulation and nonlinear factor (see equation (6)), i.e., the tumor cell concentration is chemically coupled to the immune rate β [7, 46]. Moreover, in lncRNA MALAT1 regulation, the noise of these two kinds would be not independent, so there would exist some correlation between them [26]. In fact, the analytic solution for aFPE (equations (10)–(17)) is the function of CT (τ_3) and CS (λ) between the two correlation noises $\xi(t)$ and $\eta(t)$, as well as AT ($\tau_1\tau_2$) and NS (D, α) (referring to the effective drift and diffusion terms in aFPE (equations (10)–(13)). Focusing on the regulation of CT and CS on the stationary distribution, we plot Figure 6 to decipher how the phenotypic switching occurs by varying CT and CS.

We observe from Figure 6 that by increasing the CS from −0.5 to 0.5, the probability of tumor state increases while the probability of extinction state reduces to a smaller value if other parameter values are all fixed, indicating that the CS may promote the tumor cell expression (tumor state). Hence, the positive CS means that it positively regulates the tumor cell expression, but the negative CS means that it promotes the tumor cell extinction (referring to Figure 6(a)); that is, the CS may be taken as an effective factor controlling tumor development.

The effect of the CS on cell phenotype is twofold; that is, when the multiplicative ($\xi(t)$) and additive ($\eta(t)$) noise is positively correlated (e.g., $\lambda = 0.2$, referring to Figure 6(b)) and the CT increases from 0.01 to 2 (blue to red and then to green line), the probability of extinction state decreases to near zero whereas the probability of high expression state increases. This implies that CT is a positive factor in tumor development since it promotes tumor transition and metastasis. In contrast, the negative correlation of external noise (i.e., $CS < 0$) has the opposite effect on tumor cell development. Figure 6(c) demonstrates that with increasing the CT, the probability of the tumor state decreases (from the blue line to the red to the green), but the probability of the extinction state has a significant increase. Combining Figures 6(b) and 6(c) together indicates that the development of tumor cells depends largely on the correlation of different external noise sources. This may explain why different therapeutic effects appear in the same immunotherapy. In addition, there may exist a trade-off between regulating CT and CS in tumor development, and it provides a new way to achieve cell phenotypic diversity in that CS dynamically regulates the tumor cell phenotype.

3.3. The Controllability of Mean First Passage Time (MFPT). Decoding the controllability of MFPT could quantify the effects of noises on tumor cell metastasis and transition between alternative attractors in landscape space. Here, we focus mainly on the regulation of AT/CT on tumor development to decipher the biological function of noises. According to the Krame formula, we can obtain the analytic expression of MFPT $T_{1,2} = T_{x_1 \longrightarrow x_2}$ of the system jumping from one attractor $x_{1,2}$ to another attractor $x_{2,1}$ by using the steepest descent method [71, 72], that is,

$$T_{x_1 \longrightarrow x_2} = \frac{2\pi}{\sqrt{\left|V''(x_u)V''(x_1)\right|}} \exp\left[\frac{U(x_u,t) - U(x_1,t)}{M}\right], \tag{21}$$

and similarly,

$$T_{x_2 \longrightarrow x_1} = \frac{2\pi}{\sqrt{\left|V''(x_u)V''(x_2)\right|}} \exp\left[\frac{U(x_u,t) - U(x_2,t)}{M}\right], \tag{22}$$

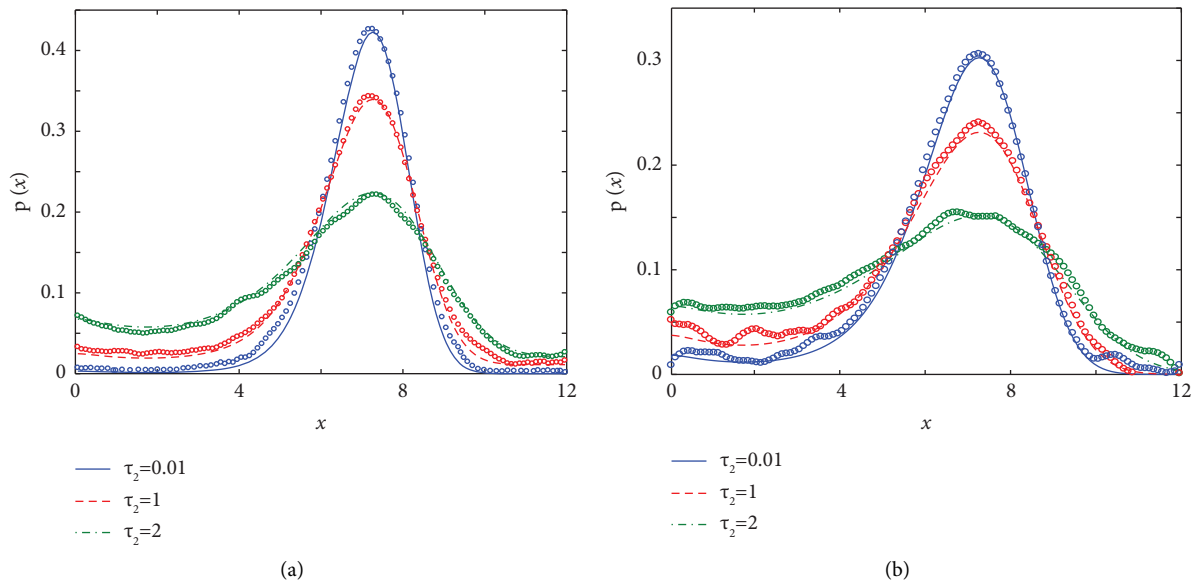

Figure 5: The regulation of AT and NS as a function of the density of tumor cells on the stationary probability distribution in an additive noise environment. (a) The NS is fixed at $\alpha = 0.2$, the AT increases from 0.01 to 2; (b) the NS is fixed at $\alpha = 0.7$, the AT increases from 0.01 to 2. The circle line represents the stochastic simulation. The other parameters are the same as in Figure 3.

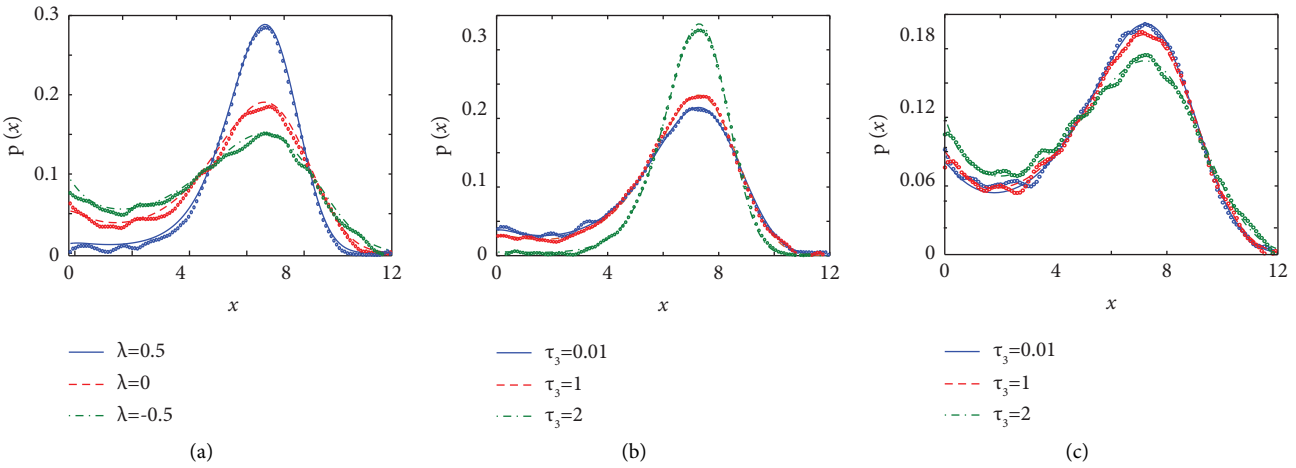

Figure 6: The regulation of the CT and CS as functions of the density of tumor cells on the stationary probability distribution in the case of two noisy sources. (a) The NS is fixed at $D = 0.8, \alpha = 0.76$, the AT is fixed at $\tau_1 = 0.4, \tau_2 = 0.2$, and the CT is fixed at $\tau_3 = 0.2$, the CS increases from −0.5 to 0.5; (b) the NS is fixed at $D = 0.8, \alpha = 0.76$, the AT is fixed at $\tau_1 = 0.4, \tau_2 = 0.2$, and the CS is fixed at $\lambda = 0.2$, the CT increases from 0.01 to 2; (c) the NS is fixed at $D = 0.8, \alpha = 0.76$, the AT is fixed at $\tau_1 = 0.4, \tau_2 = 0.2$, and the CS is fixed at $\lambda = -0.2$, the change CT is in the interval. The circle line represents the stochastic simulation. The other parameter values are the same as in Figure 3.

where V denotes the potential function defined by equation (5) U denotes the stochastic potential function (equation (16)), M is NS of the corresponding noise, and x_1 denotes the extinction state of tumor cell, while x_2 denotes the tumor state and x_u denotes critical point that is also an equilibrium state for tumor cell development (Figure 2). There exist natural restrictions on the energy barrier height for changeable parameters (i.e., $D, \alpha, \lambda, \tau_1, \tau_2, \tau_3$), that is, $\max(D, \alpha) < \Delta U = |U(x_u, t) - U(x_{1,2}, t)|$.

The numeric results of MFPT between the distinct attractors are given to exhibit the regulation of the interplay of two noises (see the above three cases). First, we investigate the effect of a single noise source, i.e., the system is in Case (i) or in Case (ii), referring to Figure 7, where Figures 7(a) and 7(b) illustrate how increasing AT (τ_1) and NS (D) of multiplicative noise regulates MFPT. Specifically, Figure 7(a) shows that the MFPT is monotonically decreasing with increasing the AT and NS with the tumor cell transition to the tumor state (x_2) from the extinction state (x_1). Also, Figure 7(b) demonstrates the inverse change tendency, and from this figure, we clearly see that the MFPT is monotonically increasing with extending AT and NS (referring to Figure S1). Meanwhile, the change of the MFPT in an additive noisy environment is nearly the same as the

multiplicative noise, referring to Figures 7(c) and 7(d). Therefore, the MFPT can be viewed as a monotonic function of the AT and NS, implying that a noisy environment may promote the state switching from the extinction state to the tumor state but suppress the inverse process. In other words, cell canceration is easier than its treatment and would need enough cost (for example, consumption of energy) to achieve the treatment. Furthermore, by comparing the subplots of Figure 7, we can see that the system has a faster response rate in the multiplicative noise case as shown in Figures 7(a) and 7(c) than in the additive noise case as shown in Figures 7(c) and 7(d) due to the difference in steepness of curves, indicating that the tumor is more sensitive to multiplicative noise than additive noise or that the multiplicative noise environment would more easily induce tumor cells.

Next, we investigate the effect of two interplaying noisy sources on the MFPT. For this, consider the system of Case (iii). It shows that there is a significant difference in the MFPTs between the single noise and Case (iii) (Figure 8). Specifically, MFPT illustrating the extinction state to the tumor state is no longer a monotonic function but exhibits different behaviors, refer to Figures 8(a)–8(d). Figure 8(a) indicates that the MFPT has a peak and decreases with decreasing the CS. In fact, if the CS (λ) is fixed, the MFPT is first an increasing and then a decreasing function of the NS (D) (referring to Figures S2(a)–S2(d) for more details), i.e., the MFPT increases when the NS (D) is small but MFPT decreases when the NS (D) is greater than about 0.05. This maybe explains why the CS has double functions on cell phenotype (referring to Figure 6). However, MFPT is a monotonic increasing function of the CS (λ) with fixing the NS (D), meaning that the negative correlation between two noise sources can be viewed as an effective enhancer for achieving cell tumorigenesis due to the small MFPT. In contrast, the positive correlation between the two noise sources can be viewed as an effective repressor for inhibiting cell tumor generation due to the increasing MFPT.

Moreover, we consider the interplay between the CS (λ) and the NS (α). Figure 8 shows that the MFPT has minimum and maximum values, respectively, when the two noises are positively correlated (e.g., when λ is approximately equal to 0.5). Furthermore, the minimum value may vanish with decreasing the CS, referring to Figure 8(c). However, the CT (τ_3) always keeps the minimum value (referring to Figures 8(b) and 8(d) and Figure S2 wherein more details are shown), meaning that the time influencing the duration of the CT (τ_3) is longer than that of influencing the duration of the CS (λ). As is well known, the CT is essentially a time lag between two noisy sources (implying that the process has memory). Therefore, the above result implies that the memory effect may persist longer than limited stimuli. The combination of Figures 8(a)–8(d) indicates that the MFPT decreases when the NS (D, α) is large enough, meaning that the cells are easier to switch to the tumor in a large noisy environment.

For tumor treatment, we consider the reverse switching process of the tumor development in the complex noisy environment, referring to Figures 8(e)–8(h). Note that because of the interplay of the CS (λ) and the NS (D, α), the dynamic behavior of the MFPT all depends on the CS (λ); that is, when the correlation of both noises is positive, the MFPT is first an increasing and then a decreasing function of the NS (D, α), but when the correlation is negative, the MFPT is always a decreasing function of the NS (D, α) (referring to Figures 8(e) and 8(g) and Figures S2(e) and S2(g) wherein more details are provided), meaning that the tumor development can exhibit different dynamic characteristics, which would explain why the stationary probability distribution has quite different change trends regulated by the CS (Figures 6(b) and 6(c)). Although the absolute value of the MFPT is less regulated by the NS (α) than by the NS (D) (referring to Figures 8(e) and 8(g), the duration time of the peak value is longer and the response is slower than in the case of additive noise. The cost of time lag for the underlying system would be fatal to tumor treatment [3, 4]. Moreover, the regulation by the CT may amplify the time difference, referring to Figures 8(f) and 8(h), which shows that the curve of the MFPT has a maximum value but the surface has a smaller curvature and a larger steepness than the case of additive noise. Therefore, the tumor state switching from a high state to a low state is more sensitive to multiplicative noise, but whether this is a reason for treatment needs to be confirmed by clinical tests [3, 53, 73].

3.4. Energy Consumption of Phase Transition Regulated by AT/CT. To dissect the internal driving mechanism of tumor transition or metastasis, we further investigate what is the cost of keeping the tumor stable and whether there is a cost-benefit relationship for tumor development. Generally, energy consumption, measured by entropy production rate (nonnegative value), can directly measure the degree of far from equilibrium [40, 43]. The nonequilibrium or irreversible character of the stochastic process is in two ways, that is, by contact with heat baths at distinct temperatures other than one heat bath or by nonconservative forces [43, 74]. Here, the aFPE equation of the tumor system is complex (equation (10)), and the diffusive coefficient $B(x)$ is the function of the position of the particle, also regulated by NS/CS and AT/CT from the fluctuations in MATLAT1 abundance. Moreover, the fluctuation of colored noise or the existence of memory induces the system into a non-Markovian. The key step of decomposing the flux flow in distinct attractors for measuring energy consumption is to become difficult [74, 75]. Therefore, it is necessary to propose a method of an effective topology network to calculate the flux flow in each attractor.

The particle jumping in the phase space is essentially mesoscopic stochastic if the interval time is enough small. It is not suitable to use the framework of the fluctuation-dissipation theorem; here, we directly model this process in the form of a chemical-master equation (CME) to calculate the flux cycle for every steady state [76, 77]. Simply, we can compare the steady distribution of the aFPE system (equation (14)) with the stationary solution of the classic two states CME to reconstruct the biochemical reaction network in mesoscopic time scale.

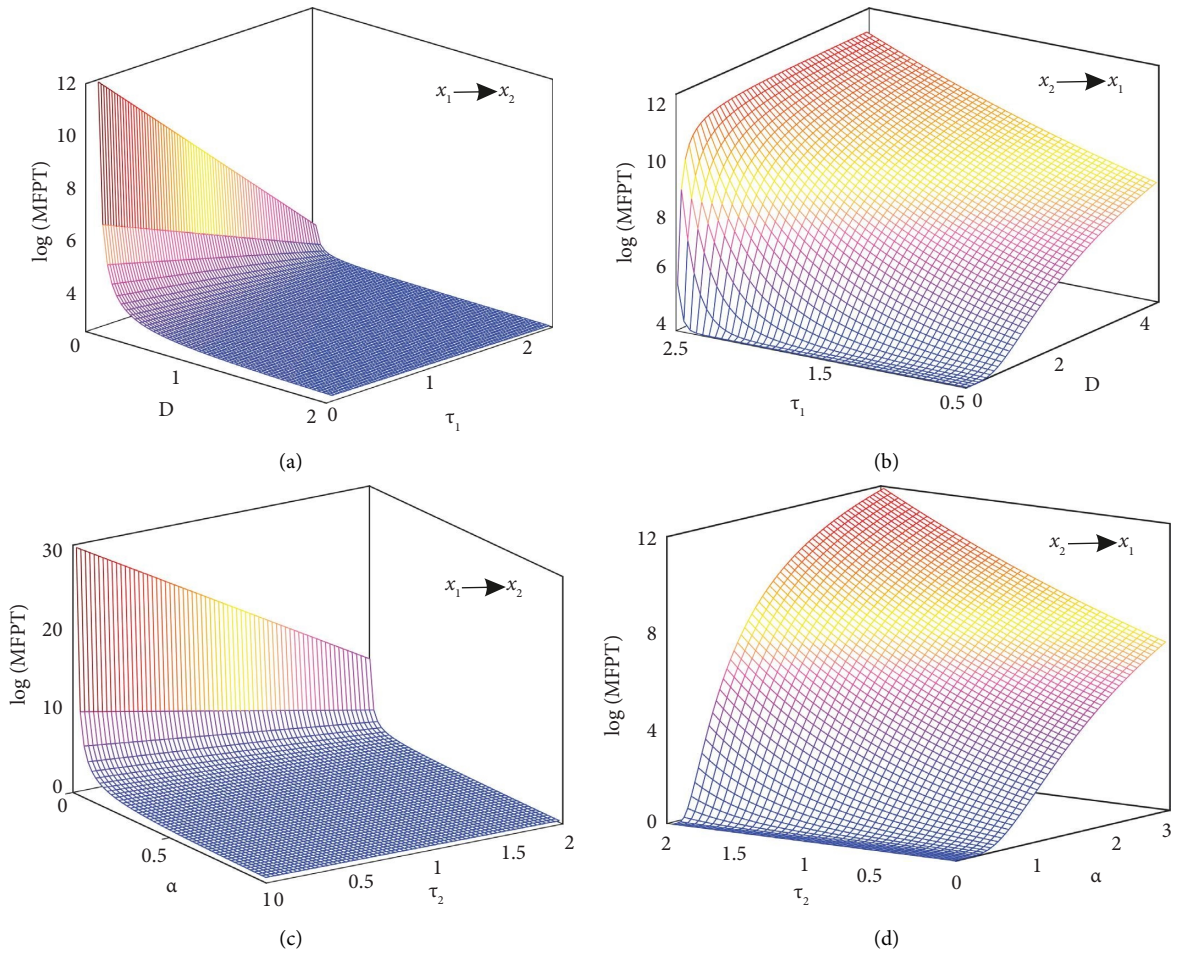

Figure 7: The mean first passage times (MFPTs) are affected by a single noisy source. (a, b) The multiplicative noise and (c, d) the additive noise. (a, c) The transition from extinction state (x_1) to tumor state (x_2) and (b, d) an inverse process. The other parameter values are the same as in Figure 3.

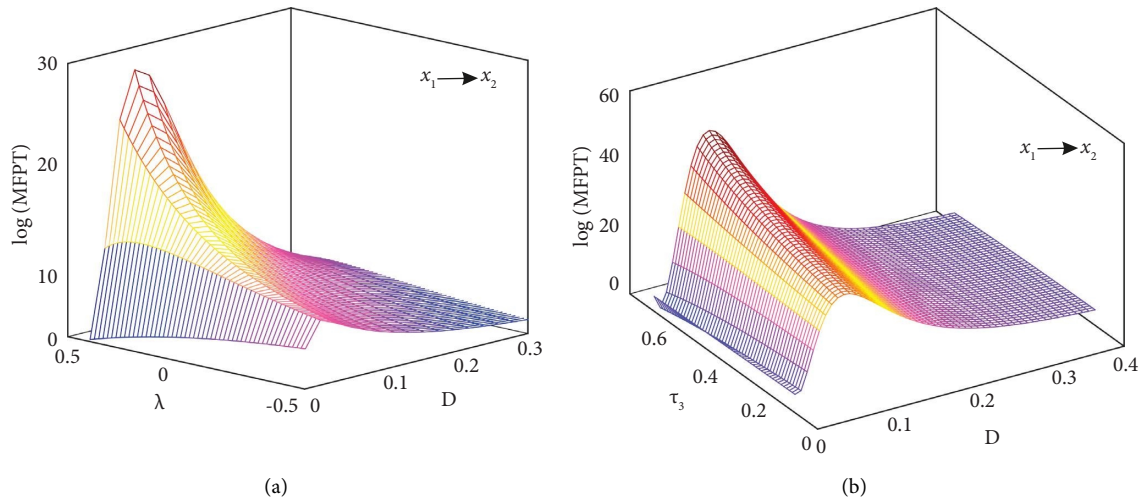

Figure 8: Continued.

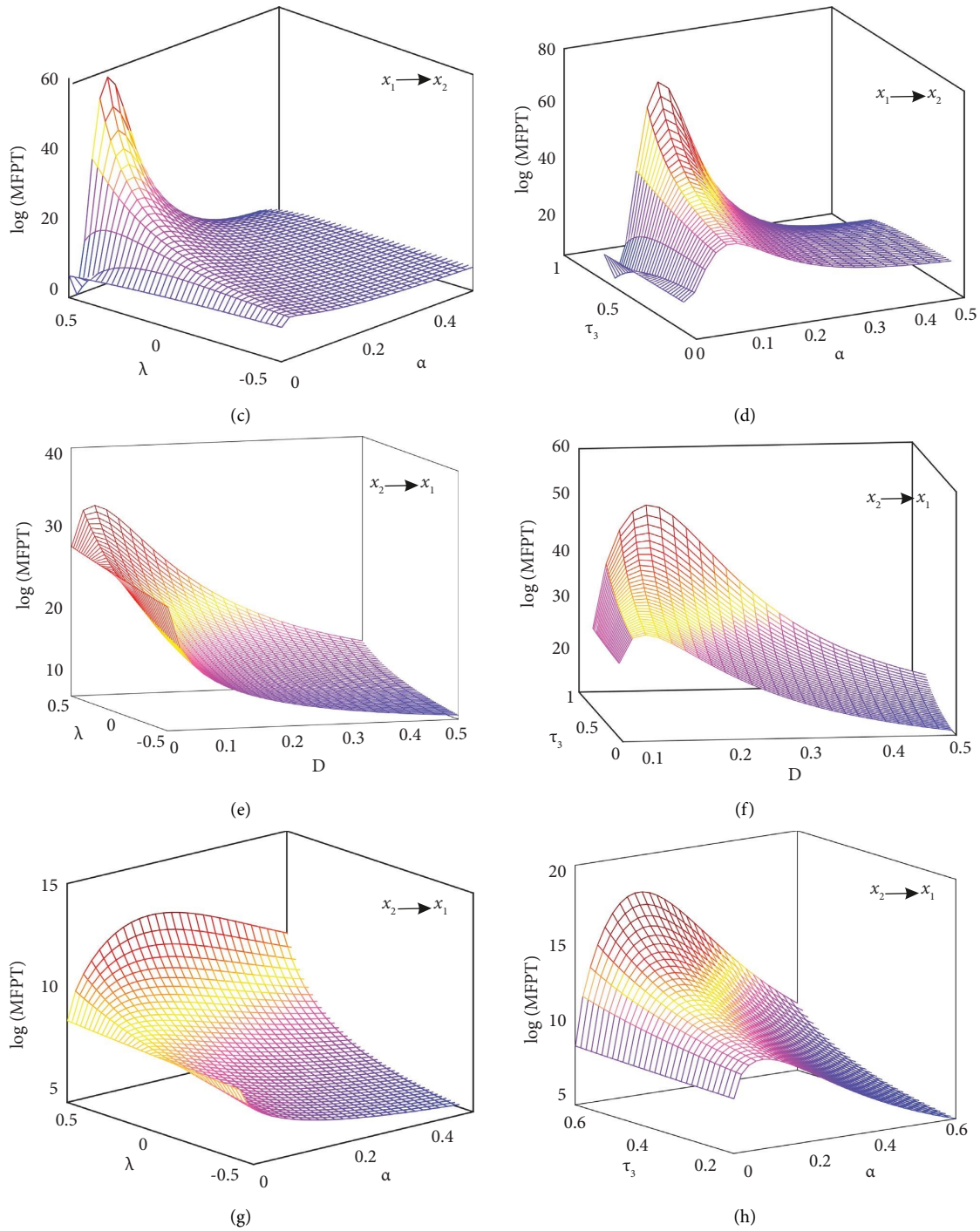

FIGURE 8: The regulation of MFPT by the interplay of the CT (CS) and NS. (a–d) The switching from a lower state (x_1) to a highly stable state (x_2), (e–h) a nearly opposite scene. (a, e) The CS (λ) and NS (D) regulate the MFPT, where parameter values are $\tau_1 = 0.1, \tau_2 = 0.1, \alpha = 0.1$, and $\tau_3 = 0.1$; (c, g) the CS (λ) and NS (α) regulate the MFPT, where parameter values are $\tau_1 = 0.1, D = 0.7$, $\tau_2 = 0.1$, and $\tau_3 = 0.1$; (b, f) the CT (τ_3) and NS (D) regulate the MFPT, where parameter values are $\tau_1 = 0.1, \tau_2 = 0.1, \alpha = 0.1$, and $\lambda = 0.5$; (d, h) the CT (τ_3) and NS (α) regulate the MFPT, where parameter values are $\tau_1 = 0.1, D = 0.5, \tau_2 = 0.1$, a$\lambda = 0.5$.

In this way, we can obtain an effective topology network for the tumor development system, and there are at least three advantages; that is, (i) it grasps the main character of our system, including switching between two stable attractors, stochastic gene expression, and some regulators from the environment, to obtain a very simpler calculating form for measuring energy cost than other results of entropy production for nonlinear FP equations, referring to Figure 9; (ii) we can unify four different types of time scales, including the force system, two types of noises, and their interaction; (iii) we transform the non-Markovian process into the framework of Markov

process, and it is possible to quantify the regulation of the noisy environment.

Without loss of generality, we define the transition rate between two stable equilibrium states to be equal to the reciprocal of MFPT and propose a stochastic system with the feedback loop, referring to Figure 9(a). The topological equivalent structure is illustrated by the following CME, which is renewed of the system (3) on a mesoscopic scale.

$$\begin{aligned}\frac{\partial P_{\text{off}}(m,t)}{\partial t} &= \sigma_u\left(E^{-1}-I\right)P_{\text{on}}(m,t)-\sigma_b(E-I)mP_{\text{off}}(m,t)\\ &\quad + d(E-I)mP_{\text{off}}(m,t)+\rho_u\left(E^{-1}-I\right)P_{\text{off}}(m,t),\\ \frac{\partial P_{\text{on}}(m,t)}{\partial t} &= -\sigma_u\left(E^{-1}-I\right)P_{\text{on}}(m,t)+\sigma_b(E-I)mP_{\text{off}}(m,t)\\ &\quad + d(E-I)\mathrm{mP}_{\text{on}}(m,t)+\rho_b\left(E^{-1}-I\right)P_{\text{on}}(m,t),\end{aligned} \tag{23}$$

where $P_{\text{off}}(m,t)$ and $P_{\text{on}}(m,t)$ denote the two factorial probabilities that the gene is in the corresponding states. According to the conservative principle of probability, we have $P = P_0 + P_1$, also given the statistical distribution of distinct attractors. It is worth mentioning that model (23) is indeed a Markovian process [22, 78], illustrating the particle jumps and resides in the neighbor hall of stable attractors.

The analytical solution of CME (23) is difficult because of the existence of nonlinear feedback, even if some simplified results have been reported [22, 78]. Four sets of parameters, transition rate, birth rate, degradation rate, and feedback strength, are included in the mesoscopic system. Here, applying the Magnus expansion constraint to the conditional mean-field approximation [44], we employ the linear mapping approximation (LMA) to simplify the CME equations (the main goal is to eliminate the effect of the nonlinearity due to the existence of feedback term) (referring to Appendix C) and to estimate effectively the parameter values. To do so, we can obtain the equivalent transition rate between two attractors $\overline{\sigma}_b = \sigma_b\langle n_p n_g\rangle/\langle n_g\rangle$ by setting the steady moment equation to zero and have

$$\overline{\sigma}_b = \frac{-1-\sigma_u+\rho_b\sigma_b+\sqrt{4\rho_u\sigma_b(1+\sigma_u)+(1-\rho_b\sigma_b+\sigma_u)^2}}{2}. \tag{24}$$

Thus, equation (19) can be reduced to

$$\begin{aligned}\frac{\partial P_{\text{off}}(m,t)}{\partial t} &= \sigma_u P_{\text{on}}(m,t)-\overline{\sigma}_b P_{\text{off}}(m,t)\\ &\quad + d(E-I)mP_{\text{off}}(m,t)+\rho_u\left(E^{-1}-I\right)P_{\text{off}}(m,t),\\ \frac{\partial P_{\text{on}}(m,t)}{\partial t} &= -\sigma_u P_{\text{on}}(m,t)\overline{\sigma}_b P_{\text{off}}(m,t)\\ &\quad + d(E-I)mP_{\text{on}}(m,t)+\rho_b\left(E^{-1}-I\right)P_{\text{on}}(m,t),\end{aligned} \tag{25}$$

yielding a steady distribution

$$P(m) = \frac{1}{m!}\frac{\mathrm{d}^m}{\mathrm{d}s^m}G(s)|_{s=-1}, \tag{26}$$

where

$$\begin{aligned}G(s) &= \frac{\exp(\rho_b s)\sigma_u}{\overline{\sigma}_b+\sigma_u}{}_1F_1\left(1+\sigma_u,\sigma_u+\overline{\sigma}_b+1,-(\rho_b-\rho_u)s\right)\\ &\quad + \frac{\exp(\rho_b s)\overline{\sigma}_b}{\overline{\sigma}_b+\sigma_u}{}_1F_1\left(\sigma_u,\sigma_u+\overline{\sigma}_b+1,-(\rho_b-\rho_u)s\right)\\ &\triangleq G_0(s)+G_1(s),\end{aligned} \tag{27}$$

and $G(s) = \sum_{m=0}^{\infty}P(m)s^m = \sum_{m=0}^{\infty}P_{\text{off}}(n)s^m + \sum_{m=0}^{\infty}P_{\text{on}}(m)s^m = G_{\text{off}}(s)+G_{\text{on}}(s)$ is a generating function corresponding to the probability distribution.

The first principle tells us that the equivalent network (equation (23)) must have the same analytical solution as that of equation (14). Equation (26) provides an effective theoretical framework to obtain the estimated value for parameters in the prespecified error bound by the nonlinear fitting [64, 65]. For the related results, one may refer to Figure S3 in Appendix E. Numeric solutions indicate that the fitting with the theoretical solution of equation (14) is well and the error is controlled. Therefore, we also calculate the factorial probabilities $P_{\text{off}}(m,t)$ and $P_{\text{on}}(m,t)$, illustrating the probability the particle dwells in each attractor. In this way, we can yield an effective Markovian jump process with discrete phase space, labeled by $\{i\}$. The transition probability of the state jumping from i to j is denoted by $k(i,j)$, and the stationary distribution of state i is denoted by $P(i)$, and we can yield directly the energy cost EP (also the entropy production rate) as follows [40, 43]:

$$\mathrm{EP} = \sum_{i,j}P(i)k(i,j)\log\frac{k(i,j)}{k(j,i)}. \tag{28}$$

Substitution into the equation (26), we have

$$\begin{aligned}\mathrm{EP} &= \sum_m P_{\text{off}}(m)\left\{\sigma_u\log\frac{\sigma_u}{\overline{\sigma}_b}+\rho_u\log\frac{\rho_u}{(m+1)d}+d\log\frac{\mathrm{md}}{\rho_u}\right\}\\ &\quad + \sum_m P_{\text{on}}(m)\left\{\overline{\sigma}_b\log\frac{\overline{\sigma}_b}{\sigma_u}+\rho_b\log\frac{\rho_b}{(m+1)d}+d\log\frac{\mathrm{md}}{\rho_b}\right\},\end{aligned} \tag{29}$$

where $P_{\text{off}}(m)$ and $P_{\text{on}}(m)$ represent the stationary distribution in two attractors (off-state and on-state), respectively. Equation (29) gives the measure of the energy cost of a particle jumping between two attractors in the nonequilibrium state.

Therefore, we investigate the energetic cost of tumor phase switching in a colored microenvironment to elucidate how energy consumption is reshaped by noise in three different cases as shown in Figure 10.

In Figure 10, we observe that by increasing the AT (τ_1) of multiplicative noise, the energy consumption increases overall, referring to Figure 10(a). However, when the NS (D)

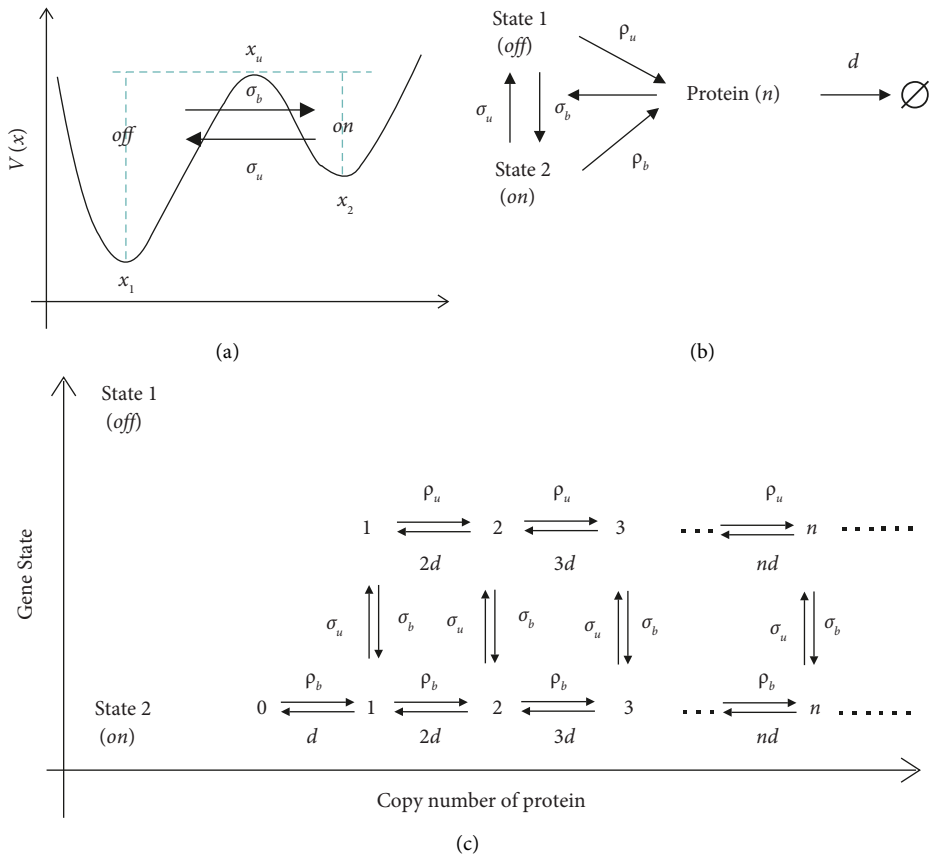

FIGURE 9: States switching and equivalent networks. (a) The tumor development switches between two stable equilibrium states, extinction state (off-state) and tumor state (on-state); (b) the corresponding CME; (c) the jumping process among the distinct states, forming a cycle flow.

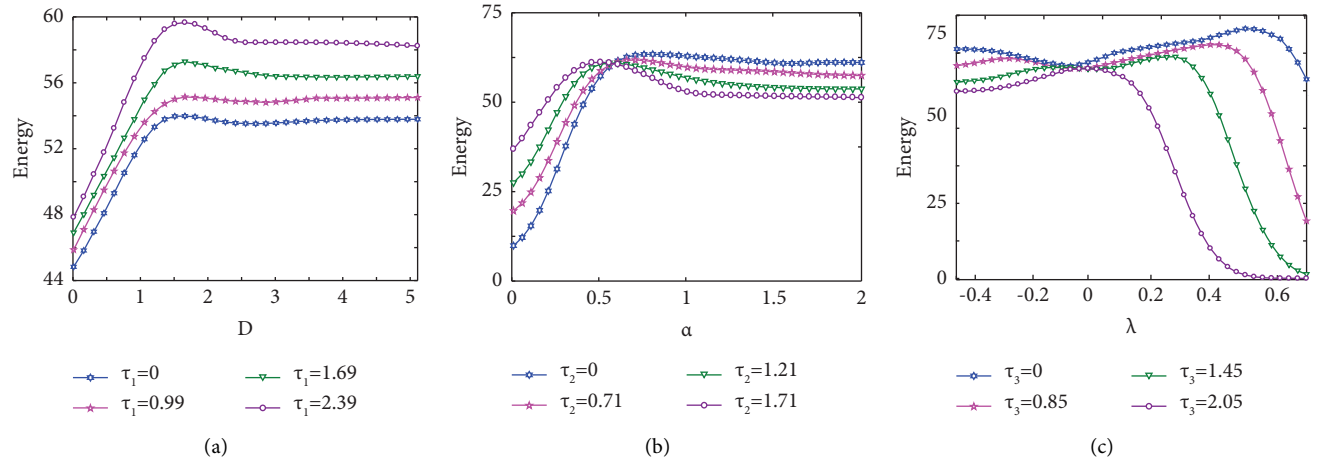

FIGURE 10: Energy cost of tumor development with different stable attractors in a colored noise environment. The case of (a–c) are corresponding to Table 1, and the parameters are set as $\tau_1 = 0.4, D = 0.8, \tau_2 = 0.2$, and $\alpha = 0.76$.

reaches a threshold (about 2), the energy consumption becomes stable. The combination of Figures 4(b) and 10(a) shows that the stochastic bistability region becomes smaller and smaller with increasing AT (τ_1), and correspondingly, the energy consumption also becomes smaller and smaller, meaning that reducing the bistable region may reduce energy consumption and the cell would cost more energy to keep bistability. However, the energy consumption has a critical point corresponding to a trade-off in the additive noisy environment, referring to Figure 10(b). This critical point (the NS is about at $\alpha = 0.7$) may directly affect the energy consumption in tumor development. When the NS

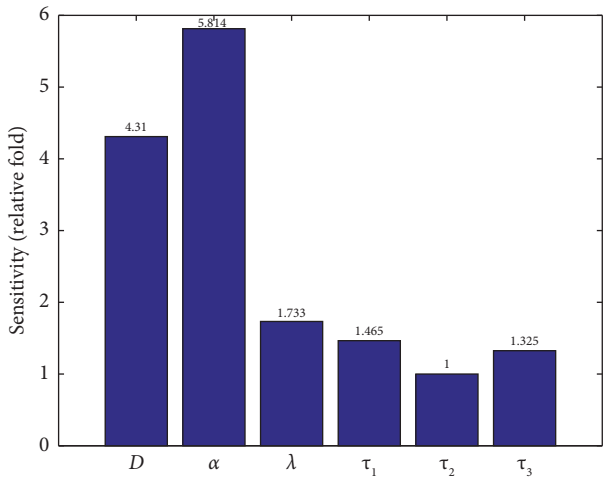

FIGURE 11: The sensitivity index defined the weighted sum of MFPT and EP, illustrating the effective regulation of every parameter.

(α) is smaller than that at the critical point, the energy consumption becomes larger and larger with increasing the AT (τ_2). Figure 5 shows that the bimodality becomes more and more apparent with increasing the AT (τ_2) when the NS (α) is fixed at a given level, meaning that the system assumes more energy to achieve the phenotypic transition of the tumor system. When the NS (α) is larger than that at the critical point, the change tendency of energy consumption is opposite to that in the case of small noise. That is, by increasing the AT (τ_2), energy consumption becomes smaller and smaller and finally tends to a stable value, referring to Figure 10(b). Since the AT (τ_2) increase may induce bimodality (refer to Figure 5(b)), a larger AT (τ_2) may reduce energy consumption even if the system phenotypes switch in a larger noise environment. This is counterintuitive because the existing results indicated that a system would consume more energy in a larger noise environment [38]. The reason why there is such a different result is that tumor development is essential to a non-Markovian process due to the AT (τ_2), that is, the AT or memory may resist extracellular fluctuations to save energy. Also, there is indeed a trade-off between energy consumption and a noisy environment mediated by the AT.

The CT (τ_3) and CS (λ) between the two noises may change the energy consumption of the tumor development system. In fact, we have known that the positive and negative CS (λ) can induce phenotypic switching and lead to presenting a different change pattern, referring to Figures 6(b) and 6(c), but the energy consumption is a decreasing function of the CT (τ_3) and has an intersection point in which the CS (λ) is equal to zero, i.e., the noisy processes are uncorrelated, referring to Figure 10(c). This means that the CS (λ) would be an effective mechanism for regulating energy consumption. Comparing the positive value with the negative value of the CS (λ) shows that the energy consumption has a little increase for a negative value of the CS (λ) but has an apparent reduction for a positive value of the CS (λ), indicating the positive CS (λ) of the two noises may induce the system to save energy consumption. The combination of Figures 6(b) and 10(c) shows that the cell phenotype may switch to the unimodal state and the probability of tumor state dominates the stationary steady distribution with increasing CT (τ_3); that is, the positive CS (λ) of noises promotes the tumor neoplasia at a lower energy dissipation. However, if the CS (λ) is negative, the energy consumption will remain at a high level because the system recovers its bimodality, and the probability of the extinction state will become larger and larger with increasing the CT (τ_3). This means that achieving the high state switching to the extinction state is at the cost of energy consumption, which may explain why the tumor is difficult to treat.

4. Conclusions and Discussions

Cancer transition and metastasis are essentially stochastic and regulated by its microenvironment characterized by extracellular noises from different sources. The fluctuations in lncRNAs would be a main noisy source of cancer development under immune surveillance [7, 64]. Recently, by ASO-mediated knock-down of MALAT1 in mouse mammary tumor virus PyMT of human luminal B breast cancer, Li et al. [7] confirmed that the fluctuation of lncRNA MALAT1 is correlated with lung cancer metastases through localizing to nuclear speckles and decreasing the elevated E-cadherin, affecting the cells invade distal lung sites. Therefore, the stochasticity of expression in MALAT1 abundance forms a colored microenvironment. Here, we propose an effective stochastic model of a cancer development system attacked by immune cytotoxic cells to investigate the mechanism of MATLAT1 marker fluctuation that regulates tumor development in two distinct ways (from time and space, achieving by regulating AT/CT and NS/CS), emphasizing cell phenotypic diversity and energy consumption. It declares that increasing AT of multiplicative noise has a dual biological function; that is, it can not only promote the tumor cells to diffuse but also make contributions to killing the cancer cells, and NS can enhance this transition. The reason why the transition can be achieved is that the stochastic bistability regime is mediated by changing the unstable attractor and NS may broaden the regime, meaning that this regulation is equivalent to the positive feedback in gene expression. While increasing AT of additive noise may reduce the steady probability of tumor state, i.e., AT may inhibit the tumor transition but NS of additive noise may attenuate this transition. However, the phenotype depends on the correlation between noises. Specifically, when CS is larger than zero (positive correlation), CT is a stimulus effective for tumor development, but it may decrease the probability of tumor metastasis if CS is negative, and there is a hedging effect between CT and CS on cell phenotype switching. Also, the positive CS may induce MFPT to have a minimum value and a maximum value, and CT always keeps a minimum value in the corresponding plane. Furthermore, tumor development regulated by noise-induced factors may consume energy to achieve cell transition and metastasis. From the viewpoint of the mesoscopic scale, we reconstruct the effective topology network in the form of CME to integrate the different time scales in tumor

development and calculate the energy cost. We show that energy dissipation depends on the type of noise. There exists a trade-off between phase transition and energy cost for additive noise by regulating NS and AT in an additive noisy environment, but extending AT of multiplicative noise may increase effectively energy dissipation; the energy cost is a decreasing function of CT, and the CS may amplify this difference, depending on its sign. These results indicate that the biological function of colored noises can be achieved in time and space scenarios by changing AT/CT and NS/CS.

Equations (10)–(14) demonstrate that the molecular memory induced by AT/CT may violate the detailed balance [53, 78, 79]. For the reduced system of tumor development, there are multiple heat baths here (referring to equation (10)), meaning the non-Markovian tumor system is drifting by driving forces at different levels and its biological function is achieved at the expense of energy [80–84]. In our model, we can meditate AT/CT and NS/CS to regulate the whole expression process, i.e., there is the third method to regulate gene expressions. For more complex expression networks, one would expect that our results here, qualitative and model-free, such as AT, can be a "fine-tuner" for phase switching at the cost of energy, still hold.

Moreover, we can define an integrative function called sensitivity index to evaluate comprehensively the regulation effect of AT/CT and NS/CS on tumor development [85–87]. $\theta = \mu_1 * 1/\mathrm{MFPT} + \mu_2 * 1/\mathrm{EP}$ is defined, where μ_1, μ_2 represents the weight coefficient and satisfies the conservation condition $\mu_1 + \mu_2 = 1$, and MFPT and EP are defined before, representing the mean first passage time and energy cost, respectively. Obviously, the system parameters $D, \alpha, \lambda, \tau_1, \tau_2, \tau_3$ can determine directly the value sensitivity index by the steady-state probability (Equation (14)) when the other conditions are the same. Of note, the time scale of two weighted indicators MFPT and EP has wide variations, and we must rescale them by dividing the minimal value of every trajectory and obtain Figure 11 (refer to Appendix D). It indicates that the sensitivity index of every regulation parameter on the phenotypic diversity is significantly different. The relative fold of regulation additive noise is up to about 5.814-fold, implying the tumor system is more effective for NS of additive noise than other noise resources (CS 1.733-fold). Also, the effect of CT can reach about 1.325-fold relative to AT of additive noise (calibration as reference 1), demonstrating that it may be an effective therapeutic schedule for tumor treatment called coherent diffraction therapy [88, 89].

Generally, gene expression may follow certain design principles for optimal evolutionary fitness [38, 90]. One of these constraints may be energy efficiency. From the perspective of evolution theory, there is a trend of evolution for genes towards resource conservation to maximize the energy available to cells for biosyntheses, growth, and division, due to the limited system of energy obtained [91]. Consistently, lots of researchers have reported that the actual evolutionary path of genes is much lower than others' path in energy landscapes to make more effective use of the energy obtained [37–39]. Owing to the trade-off between dynamic regulation and energy efficiency, this may be an optimal design, that is, the so-called minimum energy consumption principle. Of note, here, the minimum consumption is also a relative concept. Actually, the energy consumption is zero when the system is detailed balance, while the energy consumption will be positive when the system is in a nonequilibrium state. Therefore, it is interesting to decipher whether there exists an optimal path consuming the least energy to achieve the same biological function in the next research.

Moreover, the relationship between the phase transition and energy cost (as shown in Figures 4 and 10) shows that energy consumption is mainly used for broadening the stochastic bistability regime but for not maintaining relative stability, and the memory may accelerate energy dissipation, but CS may reduce energy consumption. These results imply the cell always consumes energy to achieve its phenotype adaptability, and it is also intelligent to take advantage of the correlation of the extracellular noisy environment to save energy dissipation. There may be a fitness potential landscape for tumor development in the above sense of the principle of "minimization," which is worth further investigation.

Data Availability

Data sharing is not applicable to this article as no new data were created or analyzed in this study.

Conflicts of Interest

The authors declare that they have no conflicts of interest.

Authors' Contributions

H.H.W. and L.Y.C. proposed and designed this study, performed all numerical simulations described in the paper, interpreted the results, and wrote the paper. Q.Q.L., Y.W., and H.H.W. performed an analytical treatment of a stochastic differential equation in Section II and in the supplementary material, performed preliminary numerical simulations of system (6) not illustrated in the paper but delivered rough initial results, calculated stochastic bifurcation for Figure 4, and edited the paper. Both authors contributed to the discussions. Leiyan Chen and Yan Wang contributed equally to this work.

Acknowledgments

This work was supported by the National Natural Science Foundation of China (12261028, 11961018, and 12201110), the Hainan Province Science and Technology Special Fund (ZDYF2021SHFZ231), the Natural Science Foundation of Hainan Province (120RC451 and 2019RC168), the Guangdong Basic and Applied Basic Research Foundation (2019A1515111160), the Opening Project of Guangdong Province Key Laboratory of Computational Science at the Sun Yat-sen University (2021009), and Hainan Province Innovative Scientific Research Project for Graduate Students (Qhys2022-182, Qhys2022-183), and the financially supported by Academician Shi Jianming Station of Hainan Province.

Supplementary Materials

Supplementary material contains an overview of the analysis of local dynamics of ODEs around the fixed point (section S-1), considers the approximation Fokker–Planck equation (AFPE) for the general Langevin equation (section S-2), gives the theory for effective topology network reconstruction by employing the theory of linear mapping approximation (section S-3), and exhibits three supplementary graphs including some line graphs for mean first-passage time and steady-state probability distribution fitting (section S-4). (*Supplementary Materials*)

References

[1] D. Hanahan and R. A. Weinberg, "Hallmarks of cancer: the next generation," *Cell*, vol. 144, no. 5, pp. 646–674, 2011.

[2] A. Schmitt and H. Chang, "Long noncoding RNAs in cancer pathways," *Cancer Cell*, vol. 29, no. 4, pp. 452–463, 2016.

[3] B. Vogelstein, N. Papadopoulos, V. E. Velculescu, S. Zhou, L. A. Diaz, and K. W. Kinzler, "Cancer genome landscapes," *Science*, vol. 339, no. 6127, pp. 1546–1558, 2013.

[4] M. Malumbres and M. Barbacid, "Cell cycle, CDKs and cancer: a changing paradigm," *Nature Reviews Cancer*, vol. 9, no. 3, pp. 153–166, 2009.

[5] M. C. Mormont and F. Levi, "Circadian-system alterations during cancer processes: a review," *International Journal of Cancer*, vol. 70, no. 2, pp. 241–247, 1997.

[6] T. Tian, S. Olson, J. M. Whitacre, and A. Harding, "The origins of cancer robustness and evolvability," *Integrative Biology*, vol. 3, no. 1, pp. 17–30, 2011.

[7] H. Li, S. Q. Ma, J. Huang, X. P. Chen, and H. H. Zhou, "Roles of long noncoding RNAs in colorectal cancer metastasis," *Oncotarget*, vol. 8, no. 24, pp. 39859–39876, 2017.

[8] L. Ryashko, "Sensitivity analysis of the noise-induced oscillatory multistability in Higgins model of glycolysis," *Chaos*, vol. 28, no. 3, Article ID 33602, 2018.

[9] W. Horsthemake and R. Lefever, "Noise-induced transitions; theory and applications in physics," *Chemical Biology*, vol. 39, pp. 953-954, 1984.

[10] T. Bose and S. Trimper, "Stochastic model for tumor growth with immunization," *Physical Review E*, vol. 79, no. 5, Article ID 51903, 2009.

[11] R. P. Garay and R. Lefever, "A kinetic approach to the immunology of cancer: stationary states properties of efffector-target cell reactions," *Journal of Theoretical Biology*, vol. 73, no. 3, pp. 417–438, 1978.

[12] M. B. Elowitz, A. J. Levine, E. D. Siggia, and P. S. Swain, "Stochastic gene expression in a single cell," *Science*, vol. 297, no. 5584, pp. 1183–1186, 2002.

[13] A. Sanchez and I. Golding, "Genetic determinants and cellular constraints in noisy gene expression," *Science*, vol. 342, no. 6163, pp. 1188–1193, 2013.

[14] R. Losick and C. Desplan, "Stochasticity and cell fate," *Science*, vol. 320, no. 5872, pp. 65–68, 2008.

[15] H. Maamar, A. Raj, and D. Dubnau, "Noise in gene expression determines cell fate in Bacillus subtilis," *Science*, vol. 317, no. 5837, pp. 526–529, 2007.

[16] S. Huang, G. Eichler, Y. Bar-Yam, and D. E. Ingber, "Cell fates as high-dimensional attractor states of a complex gene regulatory network," *Physical Review Letters*, vol. 94, no. 12, Article ID 128701, 2005.

[17] Q. Li, A. Wennborg, E. Aurell et al., "Dynamics inside the cancer cell attractor reveal cell heterogeneity, limits of stability, and escape," *Proceedings of the National Academy of Sciences*, vol. 113, no. 10, pp. 2672–2677, 2016.

[18] A. Ochab-Marcinek and M. A. Tabaka, "Bimodal gene expression in noncooperative regulatory systems," *Proceedings of the National Academy of Sciences*, vol. 107, no. 51, pp. 22096–22101, 2010.

[19] L. Cai, C. K. Dalal, and M. B. Elowitz, "Frequency-modulated nuclear localization bursts coordinate gene regulation," *Nature*, vol. 455, no. 7212, pp. 485–490, 2008.

[20] H. H. Wang, Z. J. Yuan, J. Liu, and S. Zhou, "Mechanisms of information decoding in a cascade system of gene expression," *Physical Review E- Statistical Physics, Plasmas, Fluids, and Related Interdisciplinary Topics*, vol. 93, Article ID 52411, 2016.

[21] D. R. Larson, "What do expression dynamics tell us about the mechanism of transcription," *Current Opinion in Genetics & Development*, vol. 21, no. 5, pp. 591–599, 2011.

[22] V. Shahrezaei and P. S. Swain, "Analytical distributions for stochastic gene expression," *Proceedings of the National Academy of Sciences*, vol. 105, no. 45, pp. 17256–17261, 2008.

[23] J. Peccoud and B. Ycart, "Markovian modeling of gene-product synthesis," *Theoretical Population Biology*, vol. 48, no. 2, pp. 222–234, 1995.

[24] M. Kærn, T. C. Elston, W. J. Blake, and J. J. Collins, "Stochasticity in gene expression: from theories to phenotypes," *Nature Reviews Genetics*, vol. 6, pp. 451–464, 2005.

[25] P. Ji, S. Diederichs, W. Wang et al., "MALAT-1, a novel noncoding RNA, and thymosin β4 predict metastasis and survival in early-stage non-small cell lung cancer," *Oncogene*, vol. 22, no. 39, pp. 8031–8041, 2003.

[26] T. Gutschner, M. Hammerle, M. Eißmann et al., "The noncoding RNA MALAT1 is a critical regulator of the metastasis phenotype of lung cancer cells," *Cancer Research*, vol. 73, no. 3, pp. 1180–1189, 2013.

[27] B. Zhang, G. Arun, Y. Mao et al., "The lncRNA Malat1 is dispensable for mouse development but its transcription plays a cis-regulatory role in the adult," *Cell Reports*, vol. 2, no. 1, pp. 111–123, 2012.

[28] J. M. Pedraza and J. Paulsson, "Effects of molecular memory and bursting on fluctuations in gene expression," *Science*, vol. 319, no. 5861, pp. 339–343, 2008.

[29] P. Hanggi, T. J. Mroczkowski, F. Moss, and P. V. Mcclintock, "Bistability driven by colored noise: theory and experiment," *Physical Review*, vol. 32, no. 1, pp. 695–698, 1985.

[30] J. Łuczka, "Non-Markovian stochastic processes: colored noise," *Chaos: An Interdisciplinary Journal of Nonlinear Science*, vol. 15, no. 2, p. 90, 2005.

[31] L. Wolf, O. K. Silander, and E. van Nimwegen, "Expression noise facilitates the evolution of gene regulation," *Elife*, vol. 4, Article ID 5856, 2015.

[32] J. J. Zhang and T. S. Zhou, "Markovian approaches to modeling intracellular reaction processes with molecular memory," *Proceedings of the National Academy of Sciences*, vol. 116, no. 47, pp. 23542–23550, 2019.

[33] T. Aquino and M. Dentz, "Chemical continuous time random walks," *Physical Review Letters*, vol. 119, no. 23, Article ID 230601, 2017.

[34] V. M. Kenkre, E. W. Montroll, and M. F. Shlesinger, "Generalized master equations for continuous-time random walks," *Journal of Statistical Physics*, vol. 9, no. 1, pp. 45–50, 1973.

[35] O. G. Berg, J. Paulsson, and M. Ehrenberg, "Fluctuations in repressor control: thermodynamic constraints on stochastic

focusing," *Biophysical Journal*, vol. 79, no. 6, pp. 2944–2953, 2000.

[36] H. Qian, "Open-system nonequilibrium steady state: statistical thermodynamics, fluctuations, and chemical oscillations," *Journal of Physical Chemistry B*, vol. 110, no. 31, pp. 15063–15074, 2006.

[37] J. Wang, L. Xu, and E. Wang, "Potential landscape and flux framework of nonequilibrium networks: robustness, dissipation, and coherence of biochemical oscillations," *Proceedings of the National Academy of Sciences of the United States of America*, vol. 105, no. 34, pp. 12271–12276, 2008.

[38] H. Qian, "The mathematical theory of molecular motor movement and chemomechanical energy transduction," *Journal of Mathematical Chemistry*, vol. 27, pp. 219–234, 2000.

[39] C. Li and J. Wang, "Landscape and flux reveal a new global view and physical quantification of mammalian cell cycle," *Proceedings of the National Academy of Sciences*, vol. 111, no. 39, pp. 14130–14135, 2014.

[40] A. Be Rut, A. Arakelyan, A. Petrosyan, S. Cili Be Rto, R. Dillenschneider, and E. Lutz, "Experimental verification of Landauer's principle linking information and thermodynamics," *Nature*, vol. 483, no. 7388, pp. 187–189, 2012.

[41] P. Mehta and D. J. Schwab, "Energetic costs of cellular computation," *Proceedings of the National Academy of Sciences*, vol. 109, no. 44, pp. 17978–17982, 2012.

[42] H. Ge and H. Qian, "Thermodynamic limit of a nonequilibrium steady-state: maxwell-type construction for a bistable biochemical system," *Physical Review Letters*, vol. 103, no. 14, Article ID 148103, 2009.

[43] J. L. Lebowitz and H. Spohn, "A gallavotti–cohen-type symmetry in the large deviation functional for stochastic dynamics," *Journal of Statistical Physics*, vol. 95, no. 1/2, pp. 333–365, 1999.

[44] Z. Cao and R. Grima, "Linear mapping approximation of gene regulatory networks with stochastic dynamics," *Nature Communications*, vol. 9, no. 1, p. 3305, 2018.

[45] D. Schnoerr, G. Sanguinetti, and R. Grima, "Approximation and inference methods for stochastic biochemical kinetics-a tutorial review," *Journal of Physics A: Mathematical and Theoretical*, vol. 50, no. 9, Article ID 93001, 2017.

[46] G. Arun, S. Diermeier, M. Akerman et al., "Differentiation of mammary tumors and reduction in metastasis upon Malat1 lncRNA loss," *Genes & Development*, vol. 30, no. 1, pp. 34–51, 2016.

[47] K. K. Wang, Y. J. Wang, S. H. Li, and J. C. Wu, "Stochastic stability and state shifts for a time-delayed cancer growth system subjected to correlated multiplicative and additive noises," *Chaos, Solitons & Fractals*, vol. 93, pp. 1–13, 2016.

[48] T. Yang, Q. L. Han, C. H. Zeng et al., "Transition and resonance induced by colored noises in tumor model under immune surveillance," *Indian Journal of Physics*, vol. 88, no. 11, pp. 1211–1219, 2014.

[49] F. Nani and H. I. Freedman, "A mathematical model of cancer treatment by immunotherapy," *Mathematical Biosciences*, vol. 163, no. 2, pp. 159–199, 2000.

[50] F. Michor and K. Beal, "Improving cancer treatment via mathematical modeling: surmounting the challenges is worth the effort," *Cell*, vol. 163, no. 5, pp. 1059–1063, 2015.

[51] S. Huang, "Genetic and non-genetic instability in tumor progression: link between the fitness landscape and the epigenetic landscape of cancer cells," *Cancer and Metastasis Reviews*, vol. 32, no. 3-4, pp. 423–448, 2013.

[52] K. G. Petrosyan and C. K. Hu, "Noise-induced multistability in the regulation of cancer by genes and pseudogenes," *The Journal of Chemical Physics*, vol. 145, no. 4, Article ID 45102, 2016.

[53] H. Shen and P. Laird, "Interplay between the cancer genome and epigenome," *Cell*, vol. 153, no. 1, pp. 38–55, 2013.

[54] I. Bena, "Dichotomous Markov noise: exact results for out-of-equilibrium systems. A review," *International Journal of Modern Physics B*, vol. 20, pp. 2825–2888, 2006.

[55] I. Bena, C. Broeck, and R. Kawai, "Drift by dichotomous Markov noise," *Physical Review E*, vol. 68, pp. 352–375, 2003.

[56] F. Kopp and J. T. Mendell, "Functional classification and experimental dissection of long noncoding RNAs," *Cell*, vol. 172, no. 3, pp. 393–407, 2018.

[57] J. M. Raser and E. K. O'Shea, "Control of stochasticity in eukaryotic gene expression," *Science*, vol. 304, no. 5678, pp. 1811–1814, 2004.

[58] H. Ge, H. Qian, and X. S. Xie, "Stochastic phenotype transition of a single cell in an intermediate region of gene state switching," *Physical Review Letters*, vol. 114, no. 7, pp. 078101–78101, 2015.

[59] N. Friedman, L. Cai, and X. S. Xie, "Linking stochastic dynamics to population distribution: an analytical framework of gene expression," *Physical Review Letters*, vol. 97, no. 16, Article ID 168302, 2006.

[60] P. Thomas, N. Popović, and R. Grima, "Phenotypic switching in gene regulatory networks," *Proceedings of the National Academy of Sciences*, vol. 111, no. 19, pp. 6994–6999, 2014.

[61] J. Elf and M. Ehrenberg, "Fast evaluation of fluctuations in biochemical networks with the linear noise approximation," *Genome Research*, vol. 13, no. 11, pp. 2475–2484, 2003.

[62] M. M. Hansen, W. Y. Wen, E. Ingerman et al., "A post-transcriptional feedback mechanism for noise suppression and fate stabilization," *Cell*, vol. 173, no. 7, pp. 1609–1621, 2018.

[63] S. Zambrano, M. E. Bianchi, A. Agresti, and N. Molina, "Interplay between stochasticity and negative feedback leads to pulsed dynamics and distinct gene activity patterns," *Physical Review E- Statistical Physics, Plasmas, Fluids, and Related Interdisciplinary Topics*, vol. 92, no. 2, Article ID 22711, 2015.

[64] C. Jia, L. Y. Wang, G. G. Yin, and M. Q. Zhang, "Single-cell stochastic gene expression kinetics with coupled positive-plus-negative feedback," *Physical Review E- Statistical Physics, Plasmas, Fluids, and Related Interdisciplinary Topics*, vol. 100, no. 5, Article ID 52406, 2019.

[65] T. D. Frank, "Delay Fokker-Planck equations, Novikov's theorem, and Boltzmann distributions as small delay approximations," *Physical Review E- Statistical Physics, Plasmas, Fluids, and Related Interdisciplinary Topics*, vol. 72, no. 1, Article ID 11112, 2005.

[66] P. Zhu, "Associated relaxation time and intensity correlation function of a bistable system driven by cross-correlation additive and multiplicative coloured noise sources," *The European Physical Journal B*, vol. 55, no. 4, pp. 447–452, 2007.

[67] J. Charlet, C. Duymich, F. Lay et al., "Bivalent regions of cytosine methylation and H3K27 acetylation suggest an active role for DNA methylation at enhancers," *Molecular Cell*, vol. 62, no. 3, pp. 422–431, 2016.

[68] K. Sneppen and L. Ringrose, "Theoretical analysis of Polycomb-Trithorax systems predicts that poised chromatin is bistable and not bivalent," *Nature Communications*, vol. 10, no. 1, p. 2133, 2019.

[69] R. F. Fox, "Numerical simulations of stochastic differential equations," *Journal of Statistical Physics*, vol. 54, no. 5-6, pp. 1353–1366, 1989.

[70] C. F. Dormann, "Critical transitions in nature and society," *Basic and Applied Ecology*, vol. 11, no. 5, pp. 469-470, 2010.

[71] P. Hänggi, R. Bartussek, P. Talkner, and J. Łuczka, "Noise-induced transport in symmetric periodic potentials: white shot noise versus deterministic noise," *Europhysics Letters*, vol. 35, no. 4, pp. 315–317, 1996.

[72] R. F. Fox, "Laser-noise analysis by first-passage-time techniques," *Physical Review A*, vol. 34, no. 4, pp. 3405–3408, 1986.

[73] X. Sun and B. Hu, "Mathematical modeling and computational prediction of cancer drug resistance," *Briefings in Bioinformatics*, vol. 19, no. 6, pp. 1382–1399, 2017.

[74] X. J. Zhang, H. Qian, and M. Qian, "Stochastic theory of nonequilibrium steady states and its applications. Part I," *Physics Reports*, vol. 510, no. 1-2, pp. 1–86, 2012.

[75] T. L. Hill, "Theoretical formalism for the sliding filament model of contraction of striated muscle Part I," *Progress in Biophysics and Molecular Biology*, vol. 28, pp. 267–340, 1974.

[76] M. H. Vainstein and J. M. Rub, "Gaussian noise and time-reversal symmetry in nonequilibrium Langevin models," *Physical Review E- Statistical Physics, Plasmas, Fluids, and Related Interdisciplinary Topics*, vol. 75, Article ID 31106, 2007.

[77] P. Ao and P. Ao, "Department, emerging of stochastic dynamical equalities and steady state thermodynamics from darwinian dynamics," *Communications in Theoretical Physics*, vol. 5, pp. 5–22, 2008.

[78] N. Kumar, T. Platini, and R. V. Kulkarni, "Exact distributions for stochastic gene expression models with bursting and feedback," *Physical Review Letters*, vol. 113, no. 26, Article ID 268105, 2014.

[79] C. Baker, T. Jia, and R. V. Kulkarni, "Stochastic modeling of regulation of gene expression by multiple small RNAs," *Physical Review E- Statistical Physics, Plasmas, Fluids, and Related Interdisciplinary Topics*, vol. 85, no. 6, pp. 61915–62510, 2012.

[80] J. A. Cole and Z. Luthey-Schulten, "Careful accounting of extrinsic noise in protein expression reveals correlations among its sources," *Physical Review E- Statistical Physics, Plasmas, Fluids, and Related Interdisciplinary Topics*, vol. 95, no. 6, Article ID 62418, 2017.

[81] A. Singh and P. Bokes, "Consequences of mRNA transport on stochastic variability in protein levels," *Biophysical Journal*, vol. 103, no. 5, pp. 1087–1096, 2012.

[82] A. Baudrimont, V. Jaquet, S. Wallerich, S. Voegeli, and A. Becskei, "Contribution of RNA degradation to intrinsic and extrinsic noise in gene expression," *Cell Reports*, vol. 26, no. 13, pp. 3752–3761, 2019.

[83] D. Schübeler, "Function and information content of DNA methylation," *Nature*, vol. 517, no. 7534, pp. 321–326, 2015.

[84] S. Berry, C. Dean, and M. Howard, "Slow chromatin dynamics allow polycomb target genes to filter fluctuations in transcription factor activity," *Cell Systems*, vol. 4, pp. 445–457, 2017.

[85] W. Shang, Y. Chen, H. Bi, H. Zhang, C. Ma, and W. Y. Ochieng, "Statistical characteristics and community analysis of urban road networks," *Complexity*, vol. 2020, Article ID 6025821, 21 pages, 2020.

[86] W. Shang, Y. Chen, X. Li, and W. Ochieng, "Resilience analysis of urban road networks based on adaptive signal controls: day-to-day traffic dynamics with deep reinforcement learning," *Complexity*, vol. 2020, Article ID 8841317, 19 pages, 2020.

[87] W. Shang, M. Zhang, G. Wu, L. Yang, S. Fang, and W. Ochieng, "Estimation of traffic energy consumption based on macro-micro modelling with sparse data from Connected and Automated Vehicles," *Applied Energy*, vol. 351, Article ID 121916, 2023.

[88] M. Zürch, S. Foertsch, M. Matzas, K. Pachmann, R. Kuth, and C. Spielmann, "Cancer cell classification with coherent diffraction imaging using an extreme ultraviolet radiation source," *Journal of Medical Imaging*, vol. 1, no. 3, Article ID 31008, 2014.

[89] D. K. Pleskow, L. Zhang, V. Turzhitsky et al., "Coherent confocal light scattering spectroscopic microscopy evaluates cancer progression and aggressiveness in live cells and tissue," *American Chemical Society Photonics*, vol. 8, no. 7, pp. 2050–2059, 2021.

[90] B. Schwanhäusser, D. Busse, N. Li et al., "Global quantification of mammalian gene expression control," *Nature*, vol. 473, no. 7347, pp. 337–342, 2011.

[91] M. Acar, J. T. Mettetal, and A. van Oudenaarden, "Stochastic switching as a survival strategy in fluctuating environments," *Nature Genetics*, vol. 40, no. 4, pp. 471–475, 2008.